Development and delivery of biologically optimized treatment plans in proton radiotherapy

Alejandro Carabe-Fernandez
Department of Radiation Oncology
University of Pennsylvania

Elements of Radiobiological Optimization

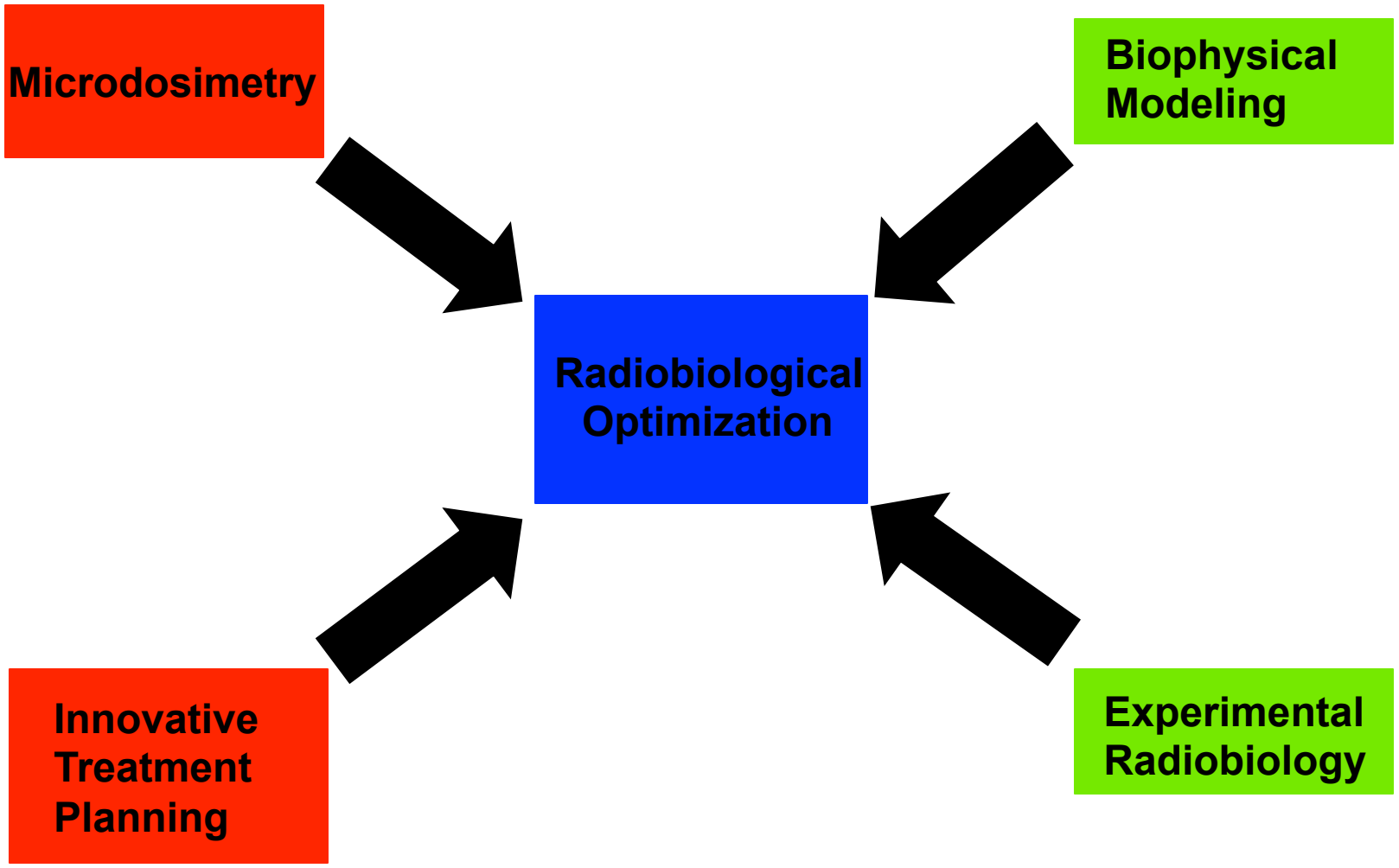

Elements of Radiobiological Optimization

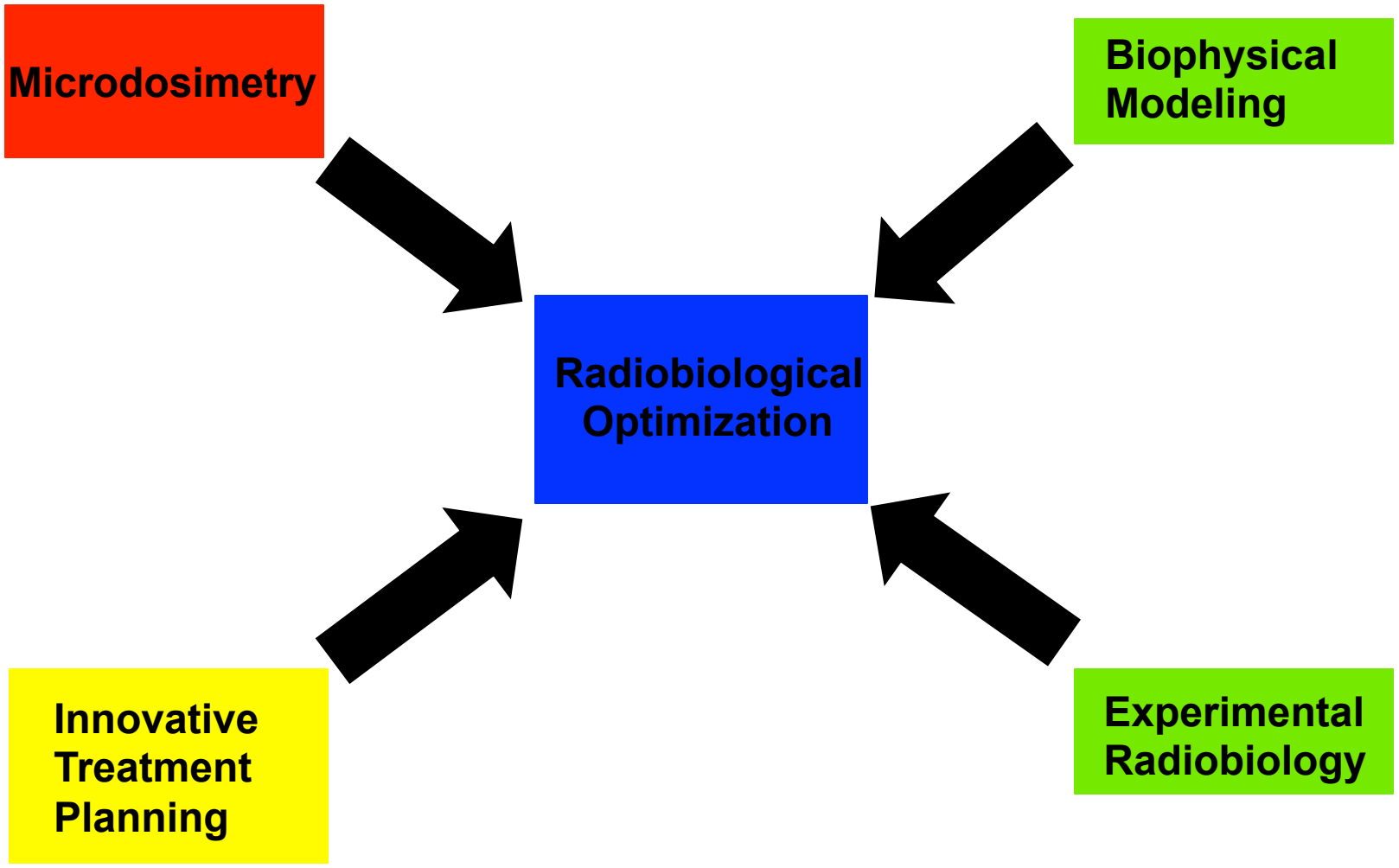

Biophysical aspects of current proton treatment planning approaches

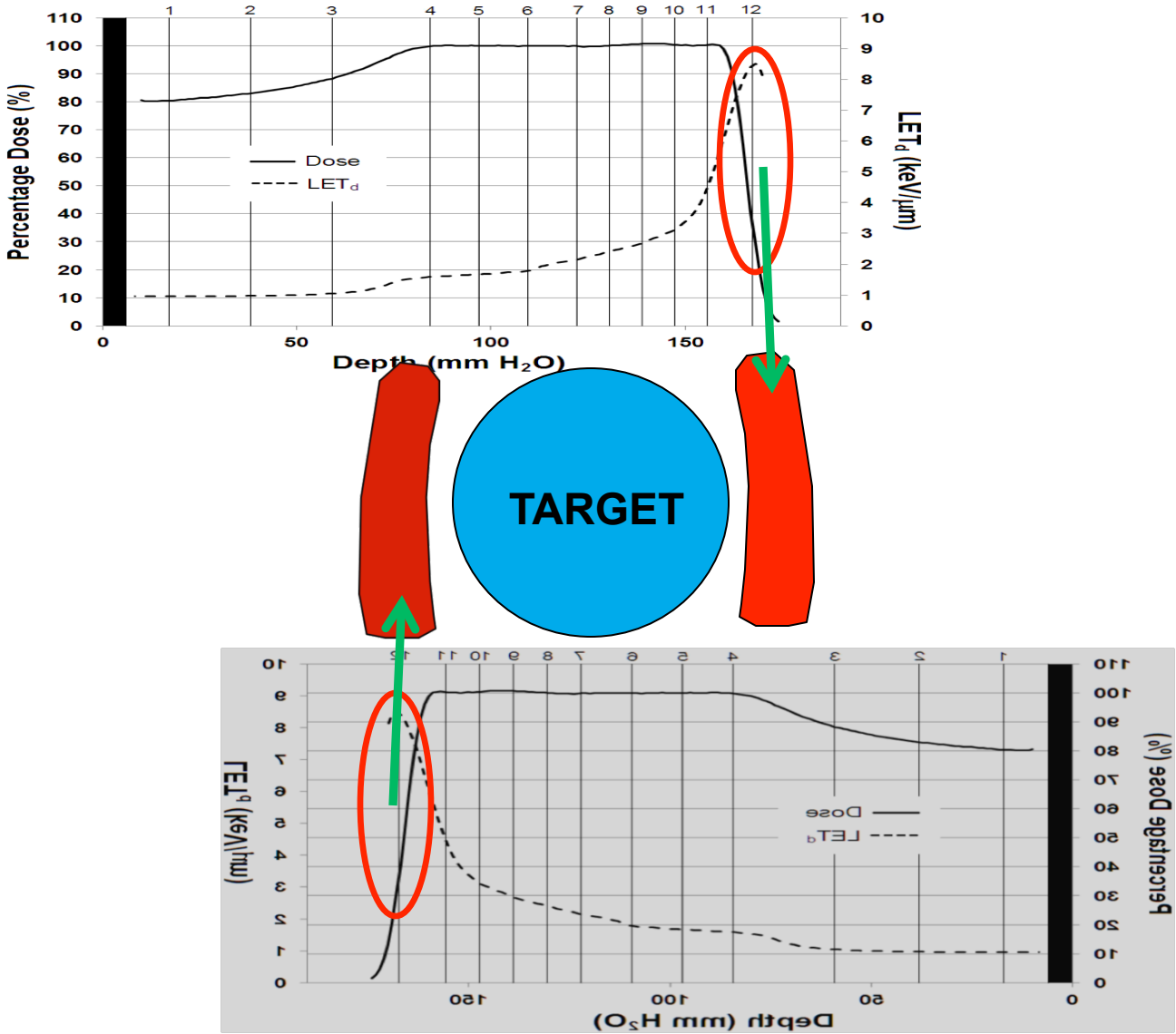

Standard treatment LET_d distributions

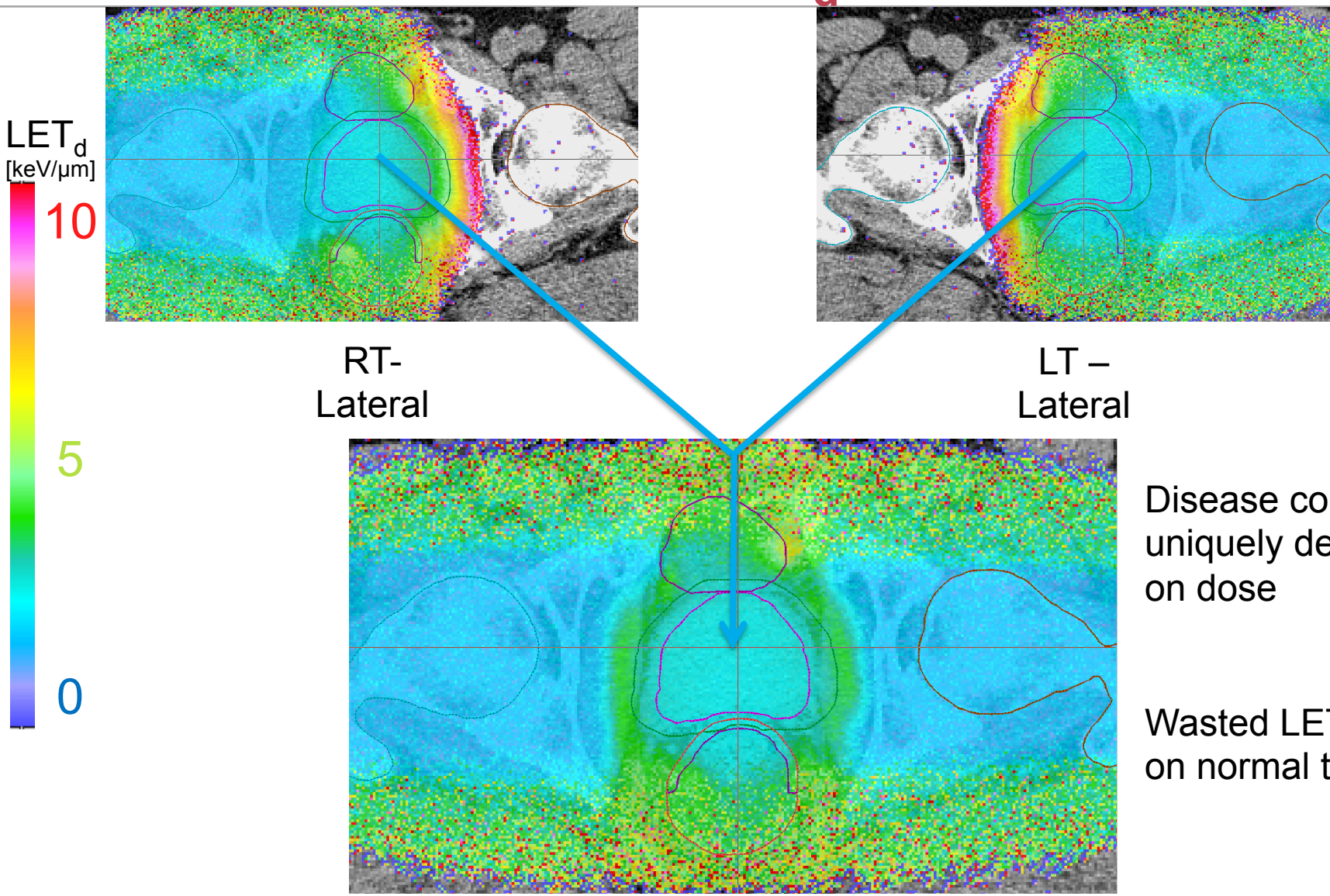

Disease control uniquely depends on dose

Wasted LET effect on normal tissue

Biophysical aspects of current proton treatment planning approaches

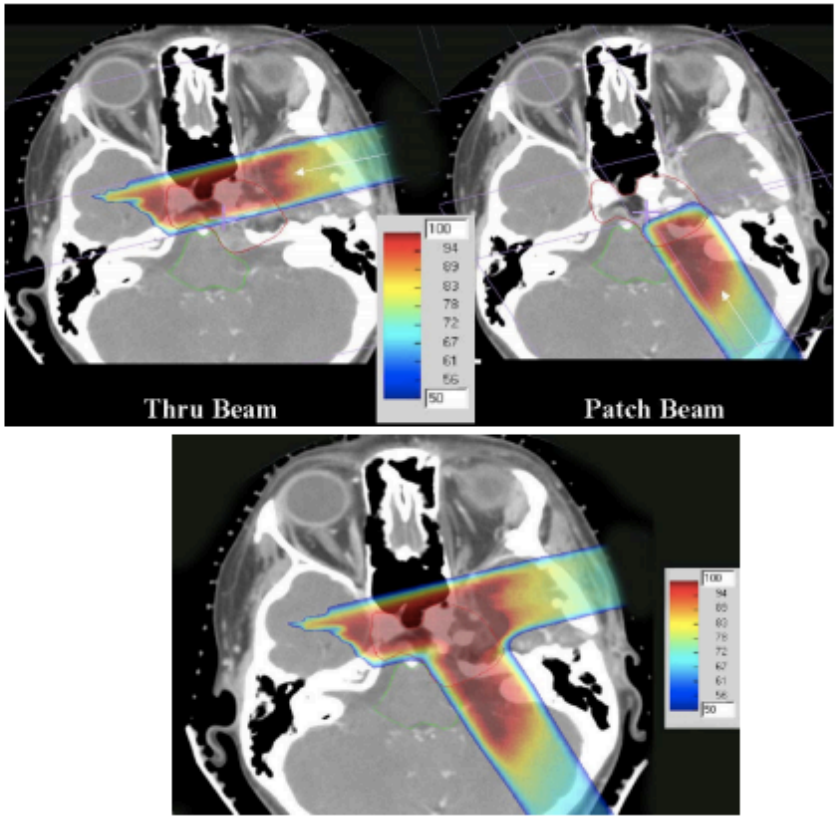

Patched Fields

Figure 13: Axial CT image with color-wash dose display resulting from thru-field which irradiates the anterior portion of the target while avoiding the brainstem and patch-field which treats the remaining portion of the target while avoiding the brainstem. The lower figure shows the combined thru/patch field combination. All doses are given in percent. (Bussiere and Adams, 2003)

Paganetti & Bortfeld
in 'New technologies in Radiation Oncology'
(Eds. Schlegel, Bortfeld, Grosu)
ISBN 3-540-00321-5 (2005)

Biophysical aspects of current proton treatment planning approaches

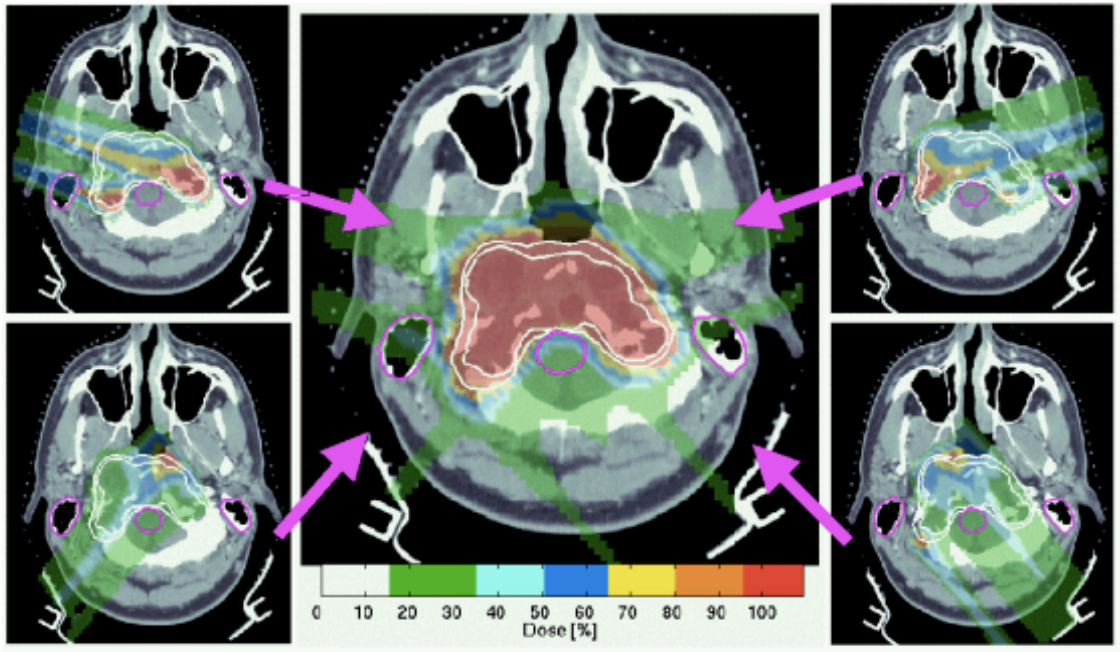

Axial CT image with color-wash dose display resulting from thru-field which irradiates the anterior portion of the target while avoiding the brainstem and patch-field which treats the remaining portion of the target while avoiding the brainstem. The lower figure shows the combined thru/patch field combination. All doses are given in percent. (Bussiere and Adams, 2003)

Paganetti & Bortfeld in 'New technologies in Radiation Oncology' (Eds. Schlegel, Bortfeld, Grosu) ISBN 3-540-00321-5 (2005)

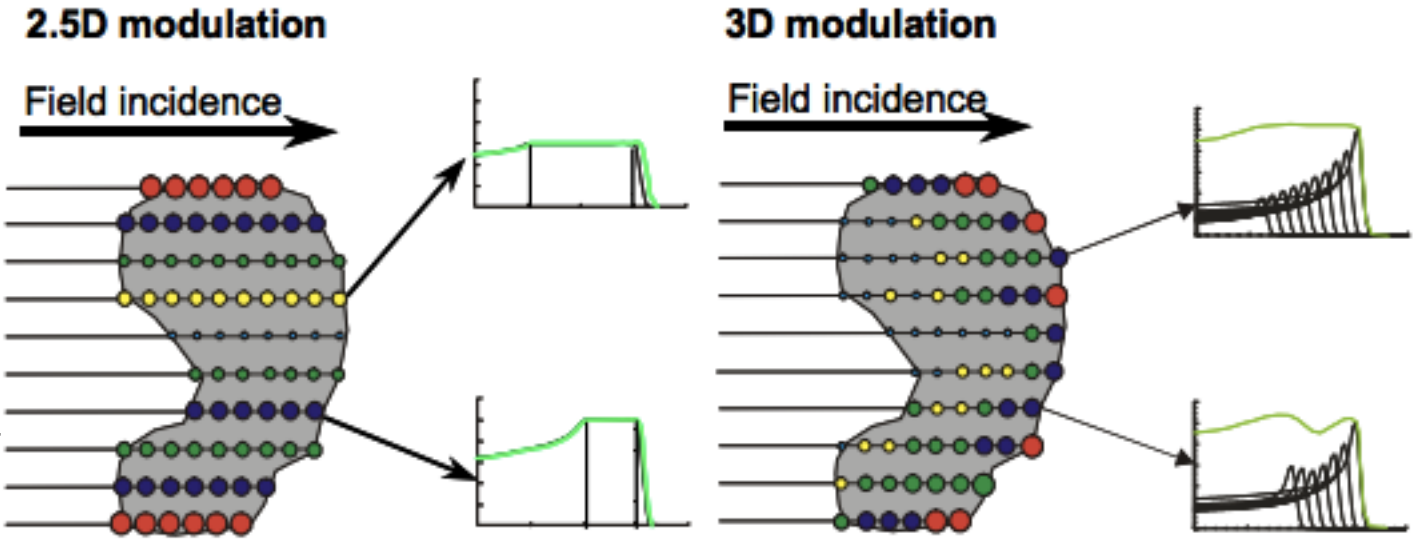

Biophysical aspects of current proton treatment planning approaches

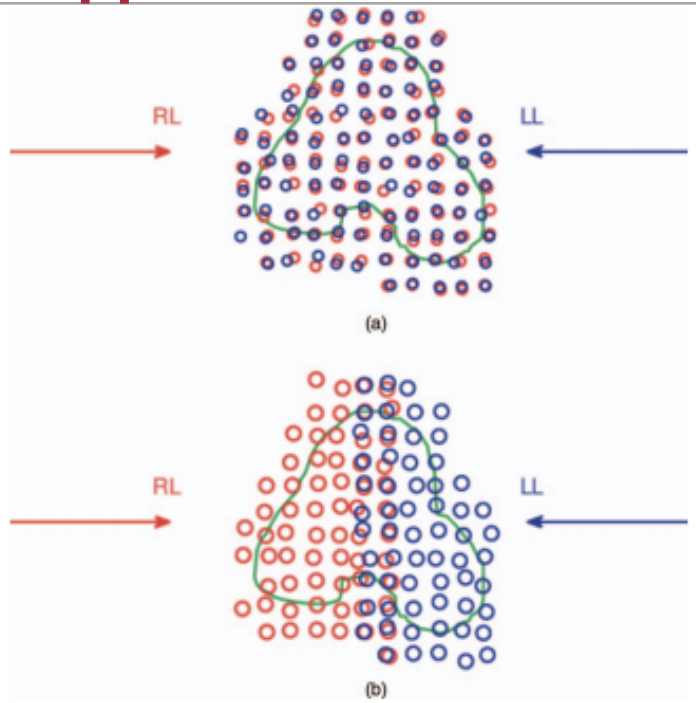

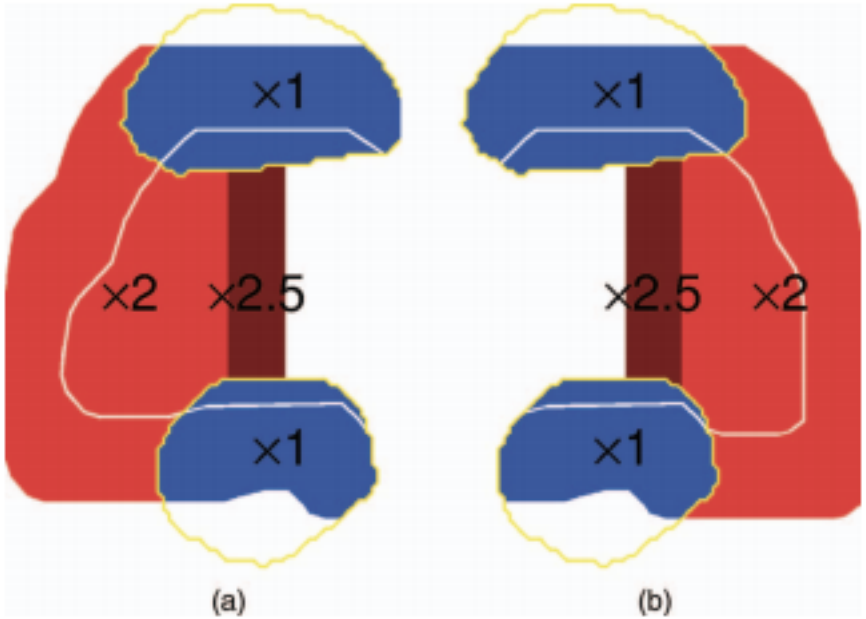

Zeng et al. Medical Physics (2013)

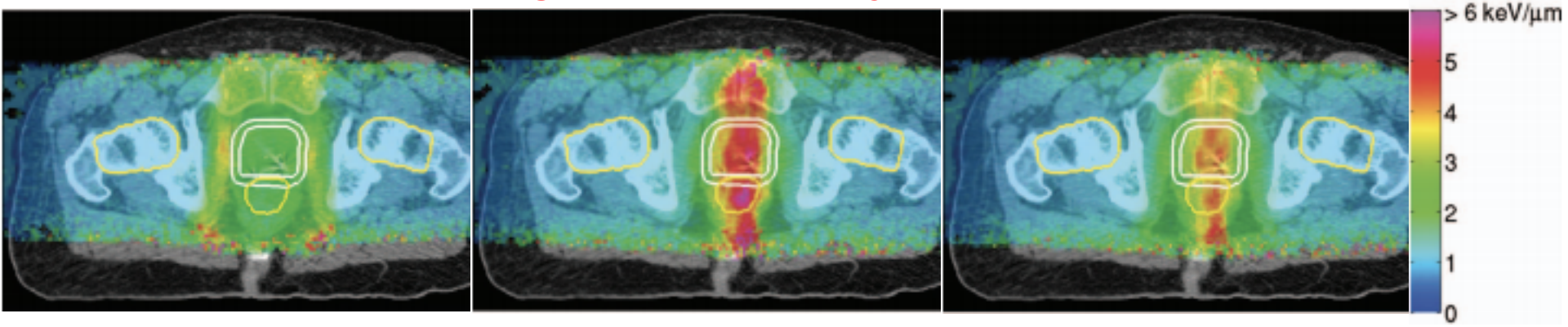

Biophysical aspects of current proton treatment planning approaches

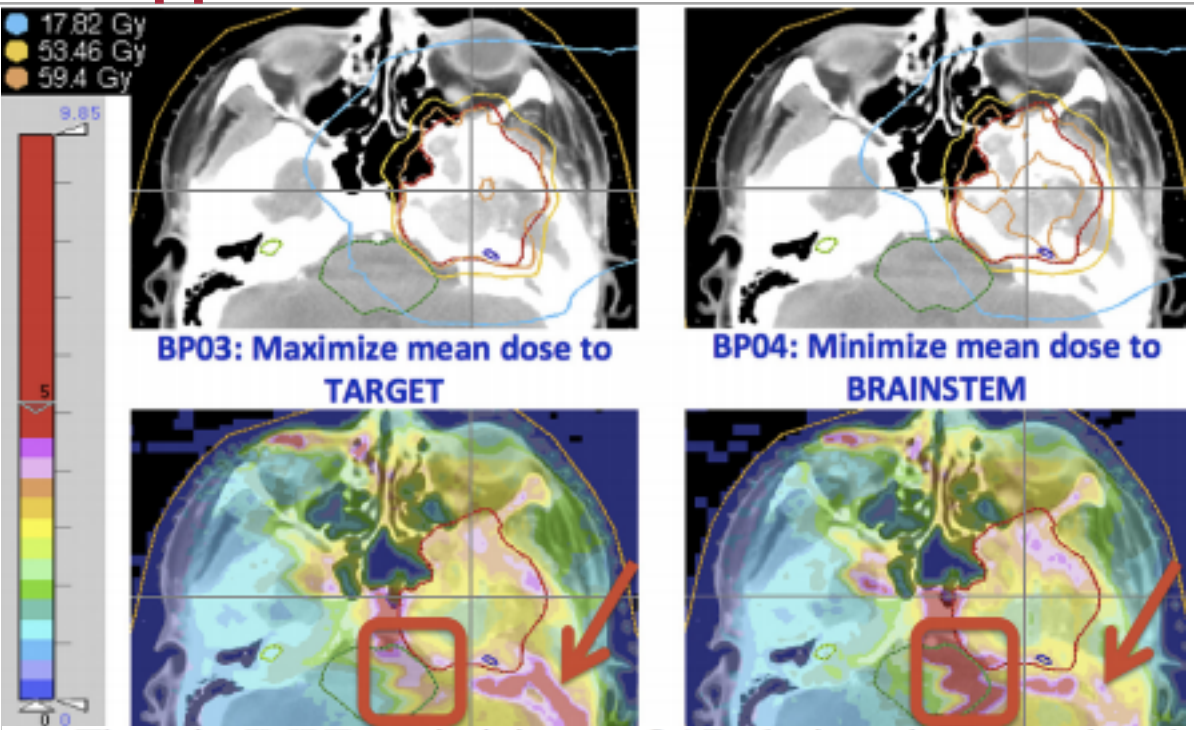

Giantsoudi et al. (2013)

Thus, in IMPT, optimizing to OAR dosimetric constraints is achieved by using the distal edge to conform the beam, yielding higher LET values, a fact currently not considered in treatment planning. The question becomes whether a decrease in (mean) dose to an OAR may be negated by an increase in (mean) LET and the associated expected increase in biological effect. To answer this question, we analyzed the RBE-weighted dose in correlation with the LET and physical dose for each structure.

Biophysical aspects of current proton treatment planning approaches

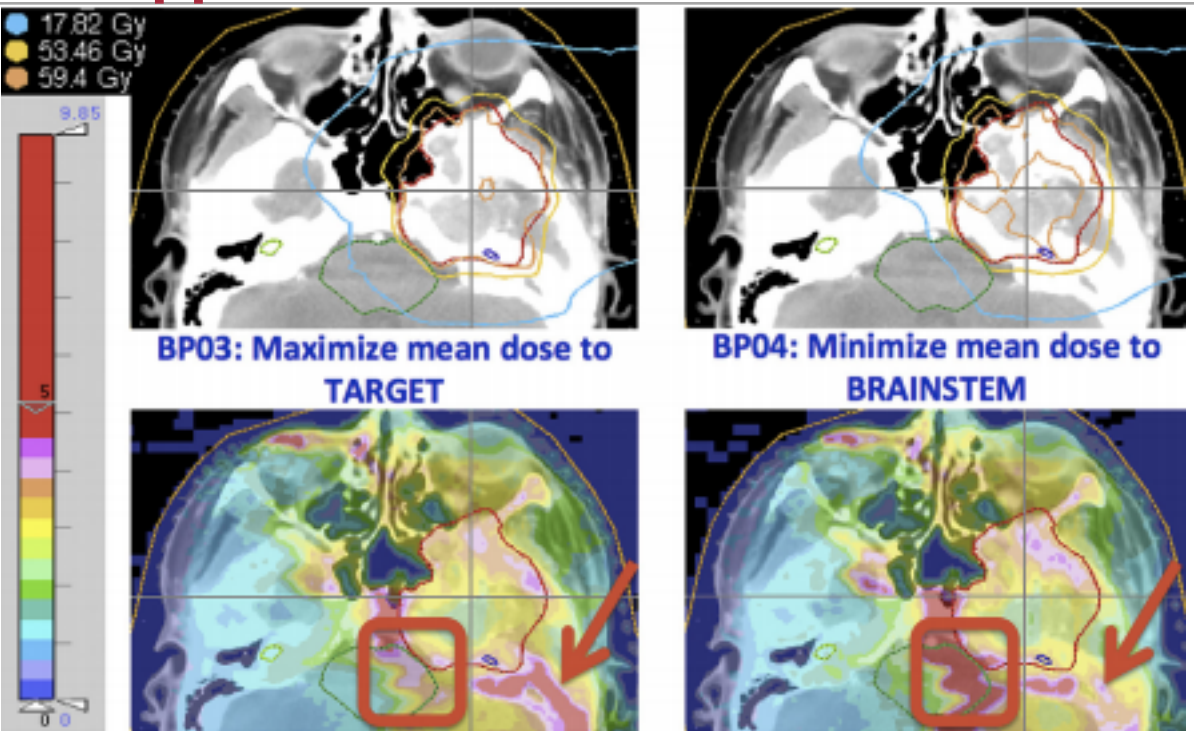

Giantsoudi et al. (2013)

Navigating the dose-optimized Pareto space, a tradeoff between low doses and low LET values for the OARs was observed, indicating the need for a method to gauge the relative importance of dose and LET to the clinical outcome of the patient. Substantial RBE variations among BPs for all patients considered in this study were associated with substantial variations in LET_{mean} values, along with variations in dose. Higher

Biophysical aspects of current proton treatment planning approaches

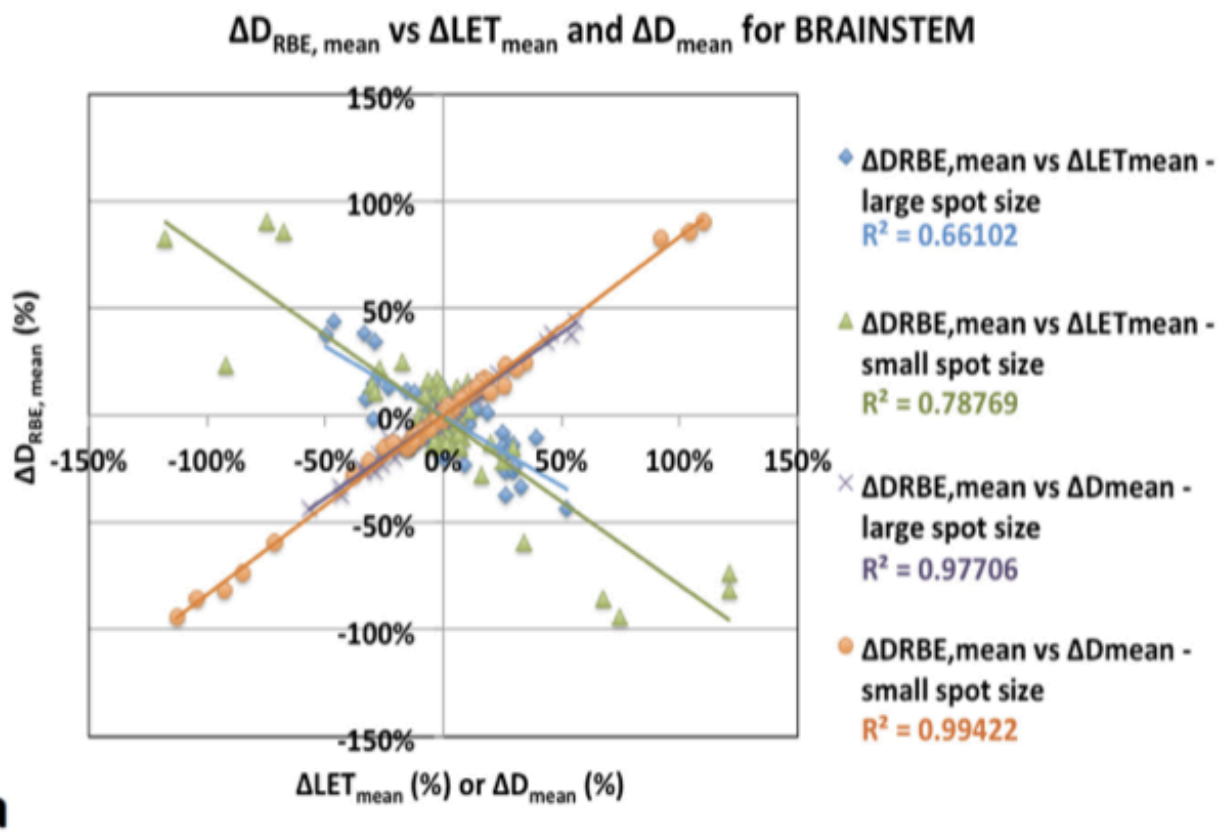

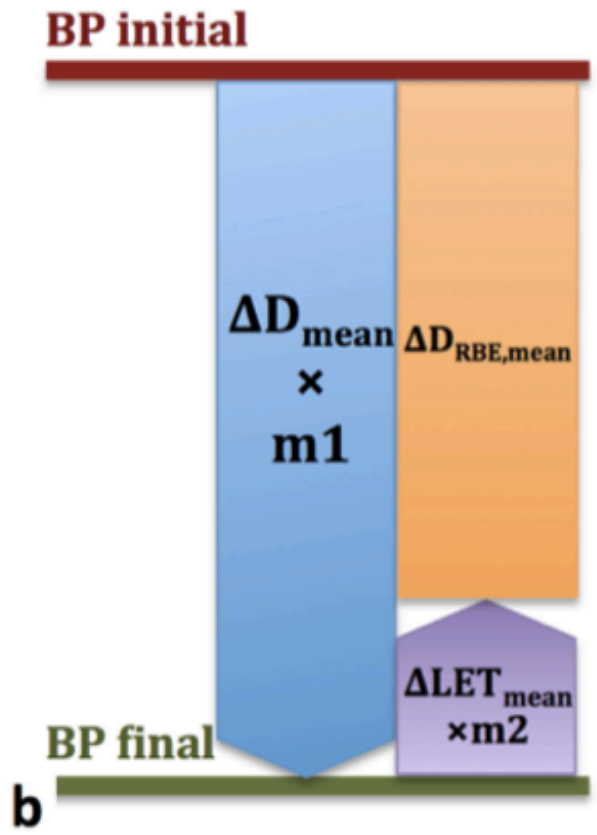

Fig. 4. (a) Plot showing how differences in mean RBE-weighted doses ($\Delta DRBE,_{mean}$) correlate with differences in mean LET (ΔLET_{mean}) and mean dose (ΔD_{mean}) values for both beam spot sizes (large: 12 mm on average; small: 3 mm on average). The R^2 values on the legend represent the coefficient of determination for each set of data. (b) Schematic diagram of Equation 3 accounting for the inverse correlation between ΔD_{mean} and ΔLET_{mean}. LET = linear energy transfer; RBE = relative biological effectiveness.

Biophysical aspects of current proton treatment planning approaches

Can we exchange dose for LET while maintaining the same biological effect in the target volume?

If we can, that would mean:

1- we could decrease the required prescribed dose (or even the number of fractions) of the treatment without loosing its biological effectiveness.

2- reduce the dose (by default from 1) in the normal tissue

3- reduce the LET in the normal tissue

Work done by: **Marcus Fager – University of Pennsylvania**

Biophysical aspects of current proton treatment planning approaches

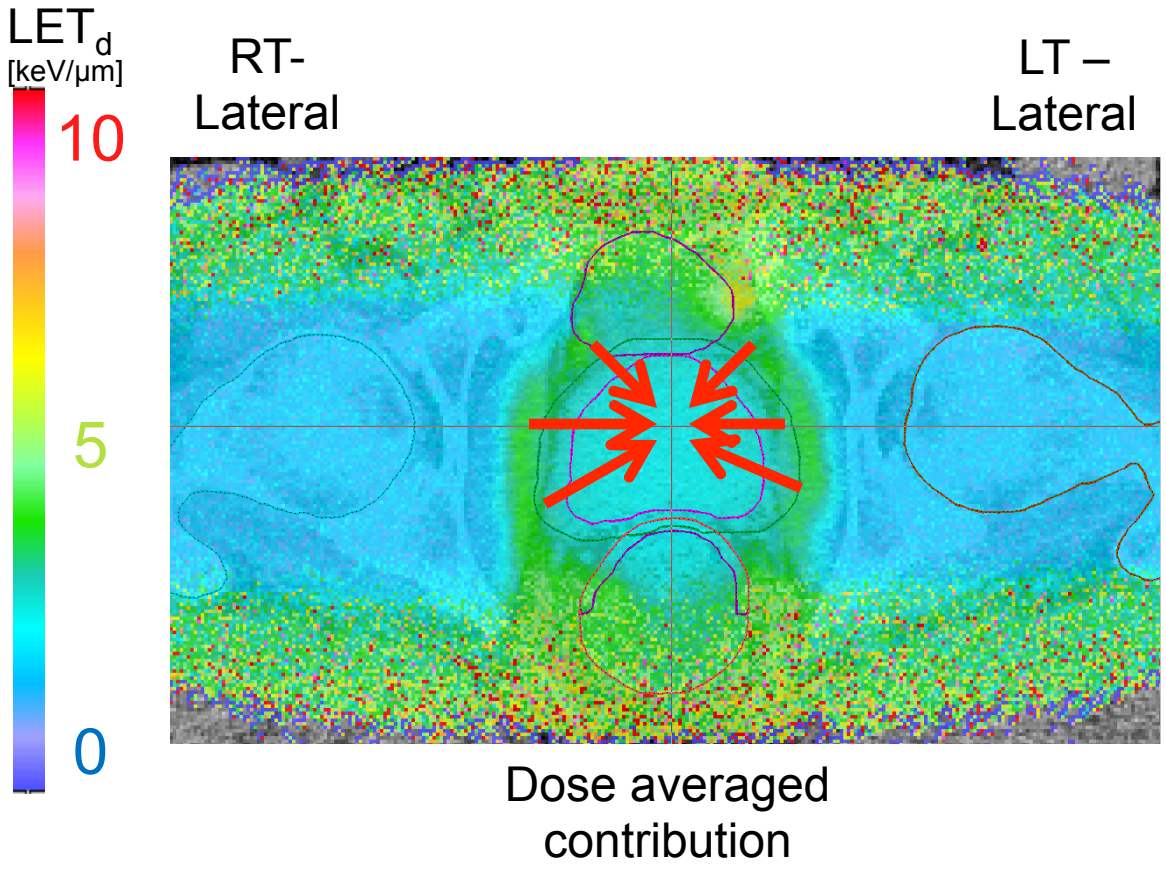

Disease control will depend on dose **and LET**

Normal tissue shielded from the region of the beam with enhanced biological effectiveness

Split Target – 2 Fields – CTV – PBSTV

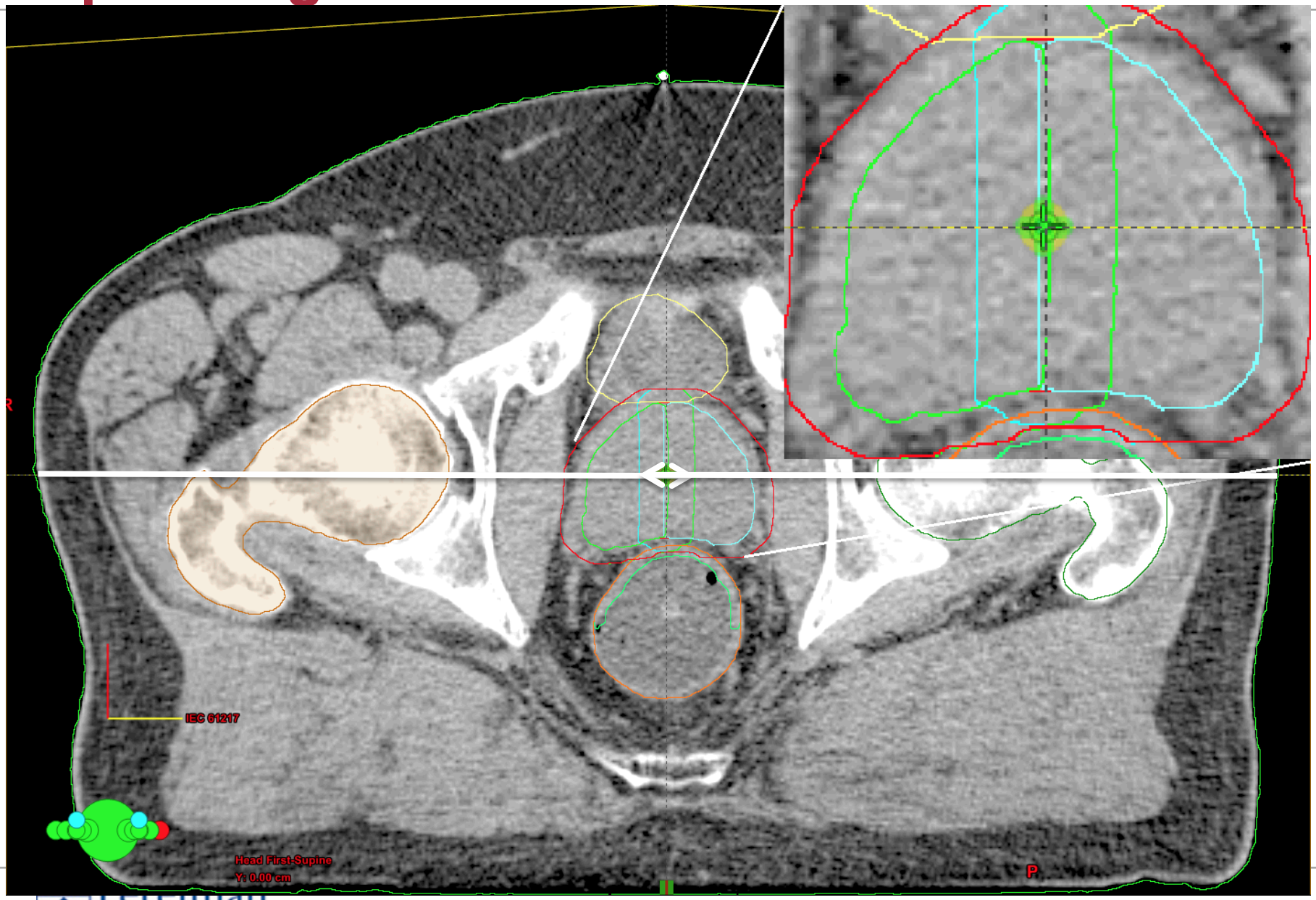

Split Target – 2 Field - LET_d distributions

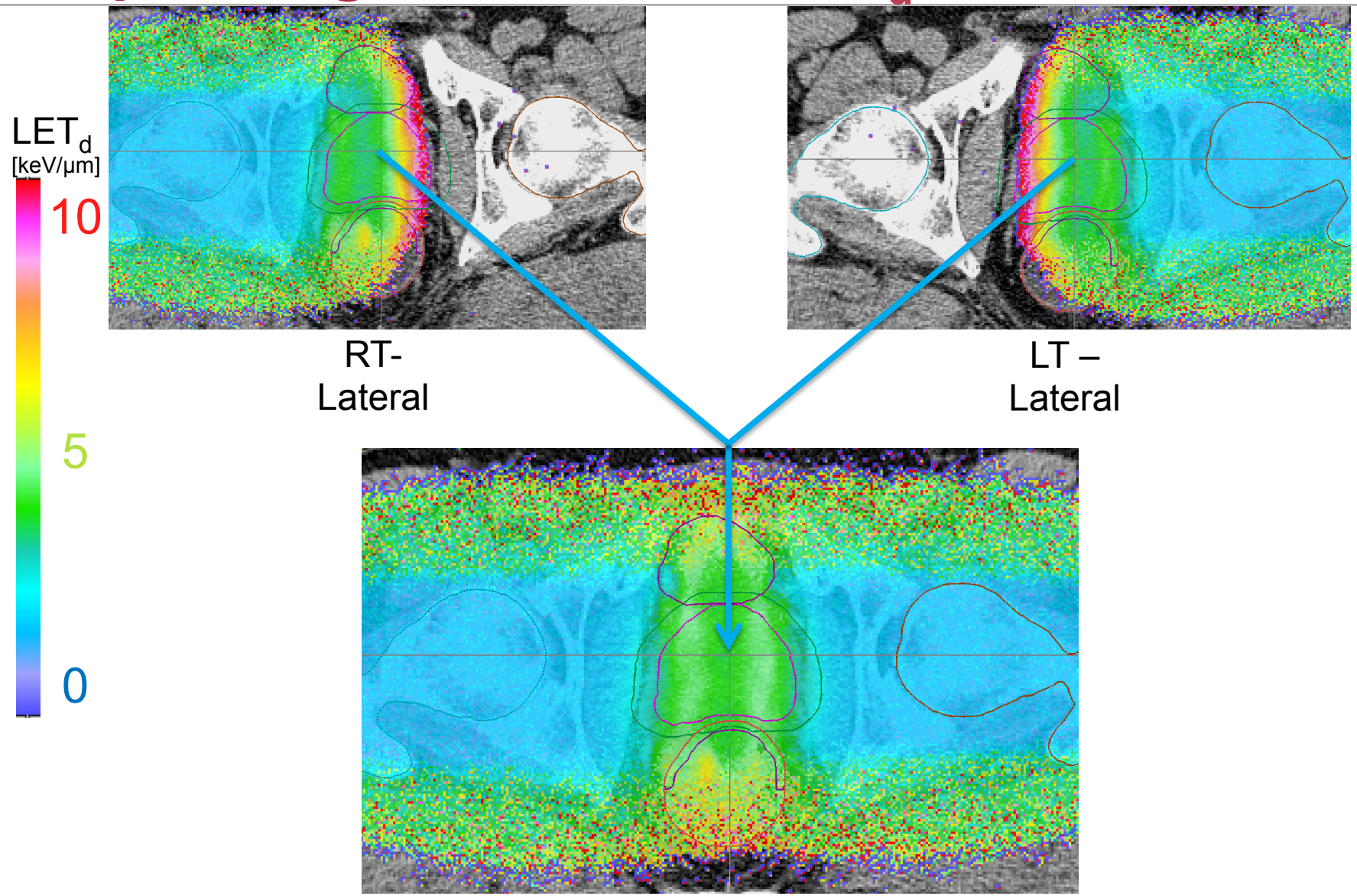

Split Target – 4 Field – CTV

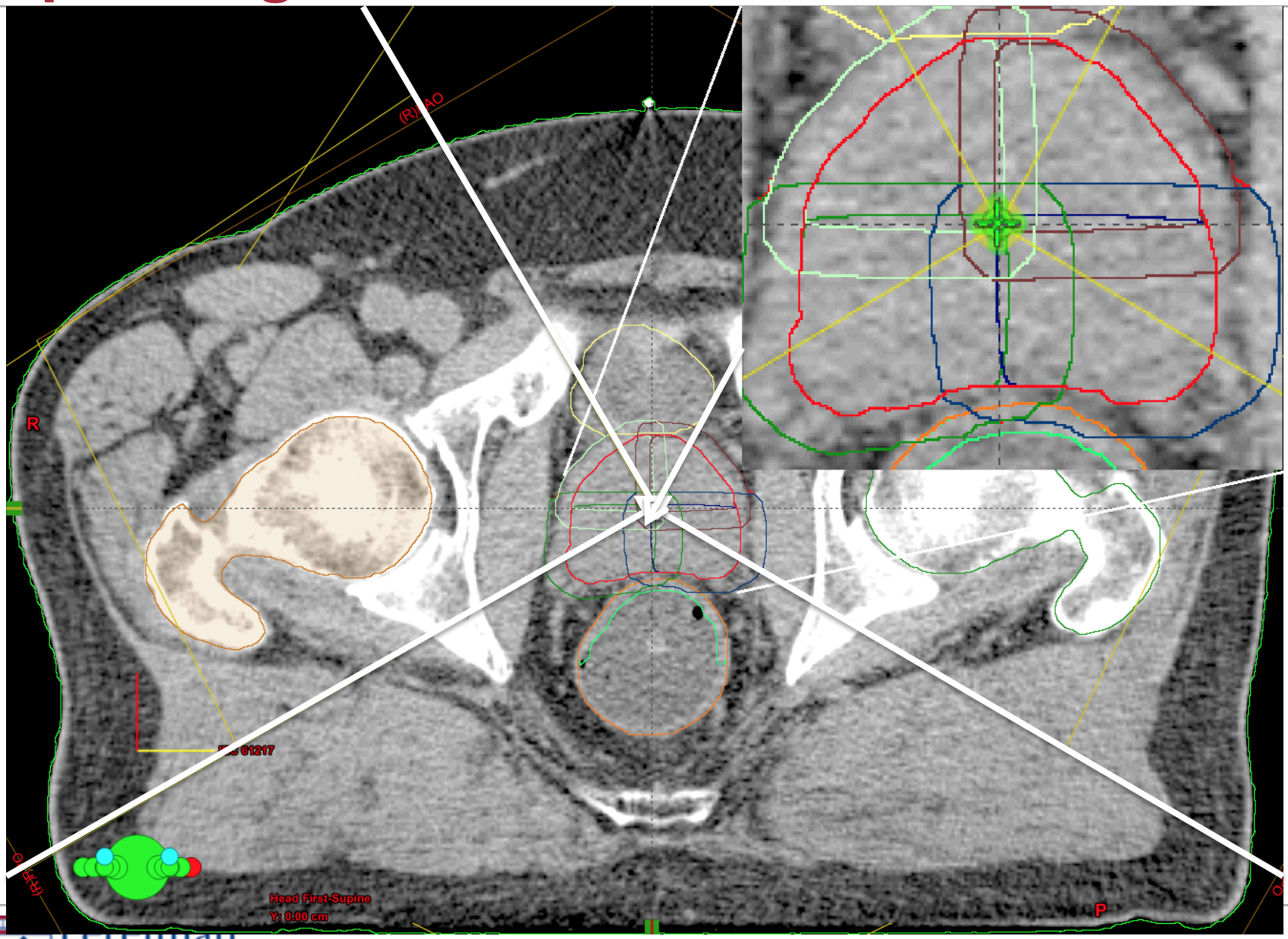

Split Target – 4 Field - LET_d distributions

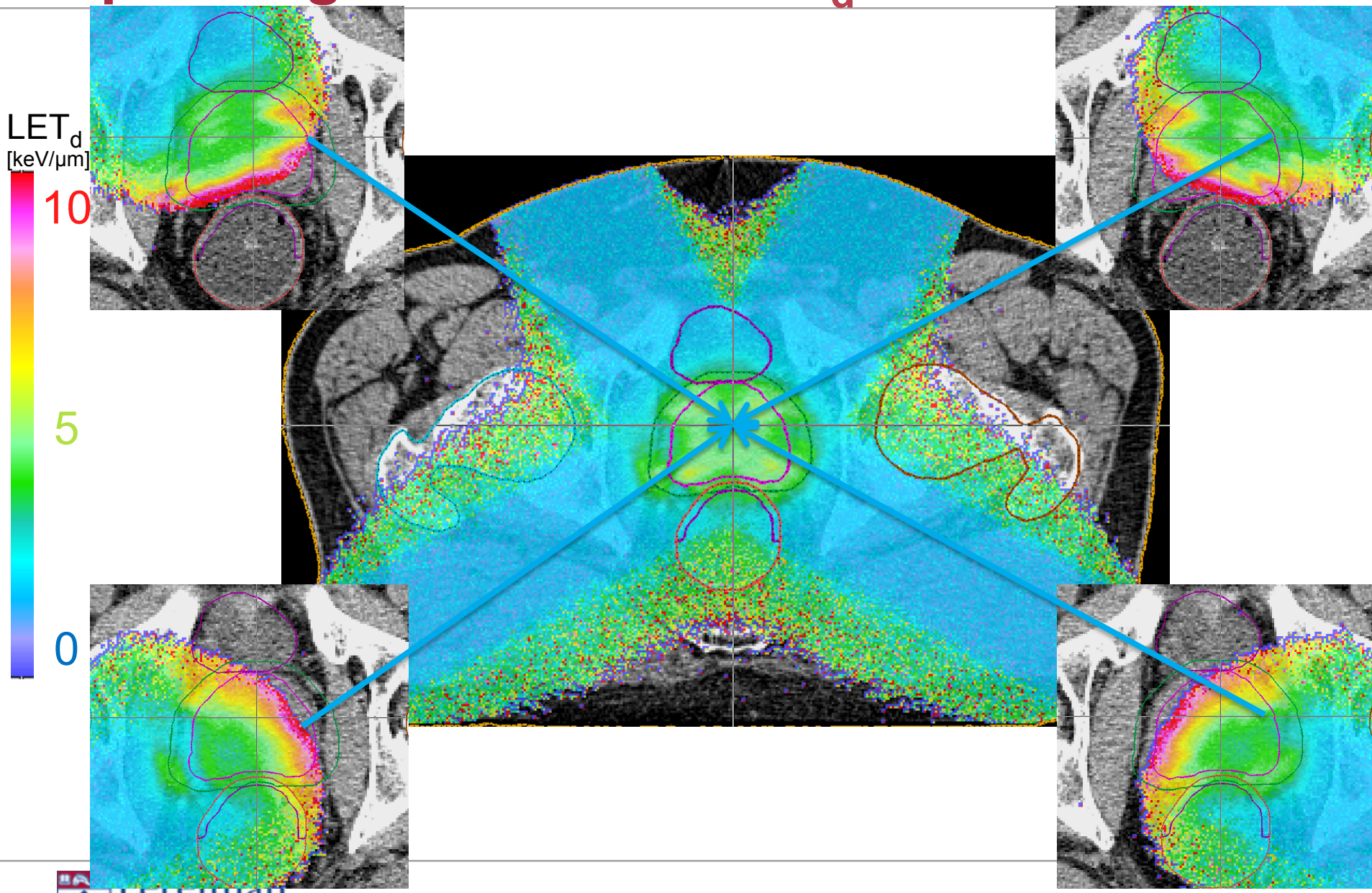

Split Target – 7 Field – CTV – PBSTV

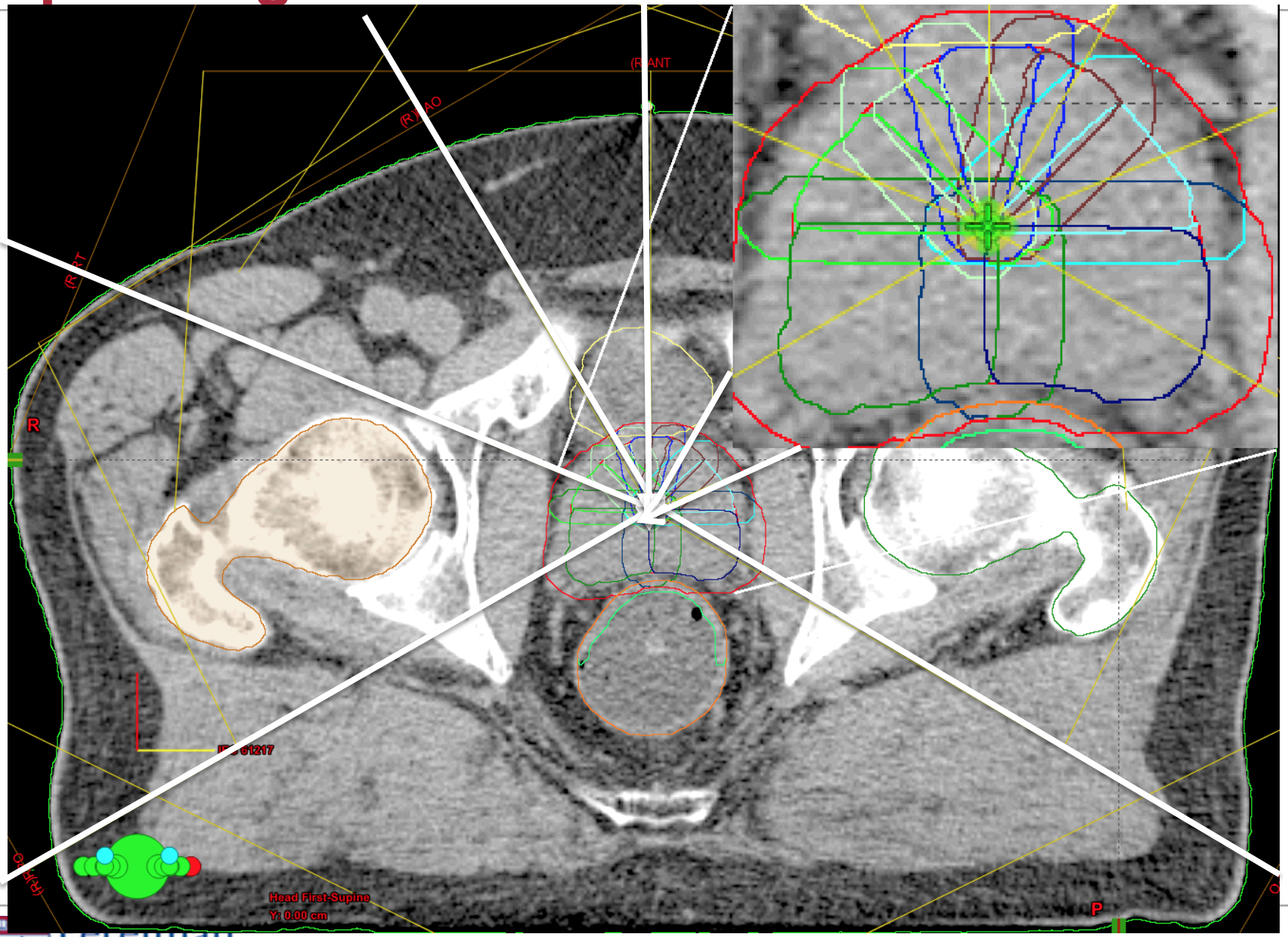

Split Target – 7 Field - LET_d distributions

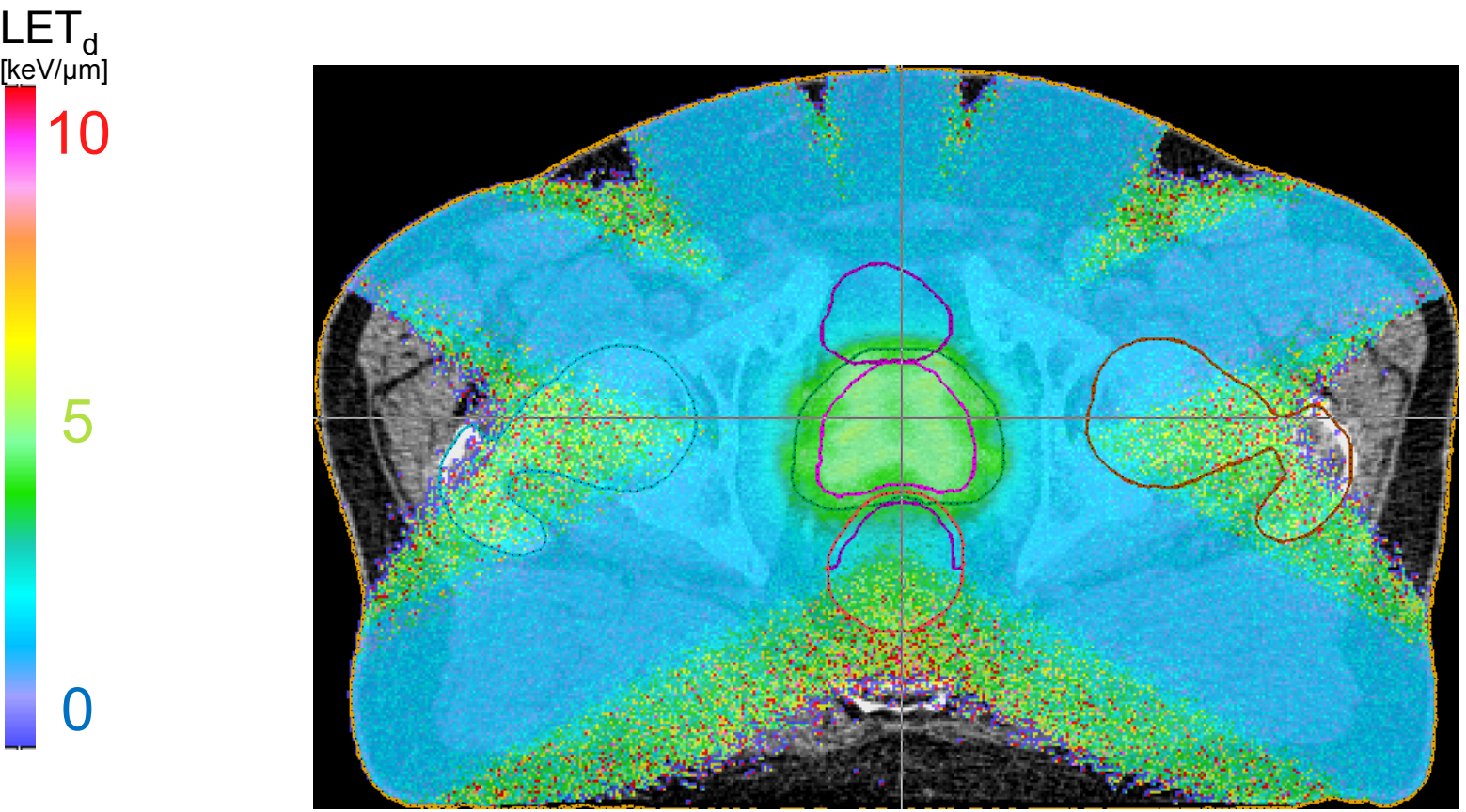

Dose Comparison

Standard Full Target

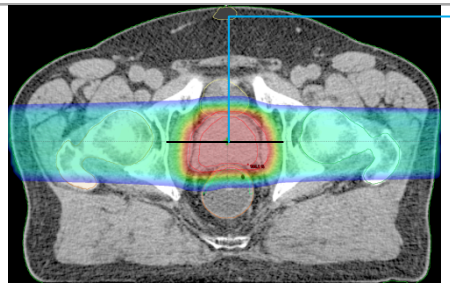

2 Field Split Target

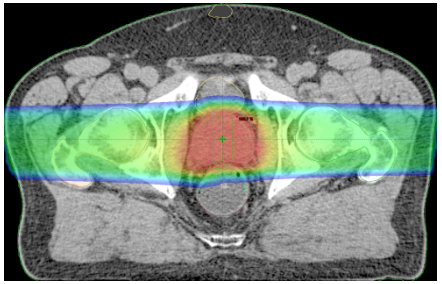

4 Field Split Target

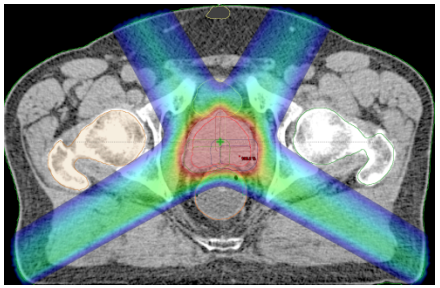

7 Field Split Target

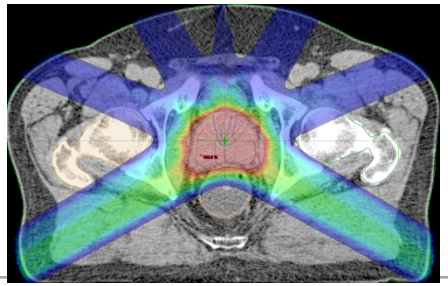

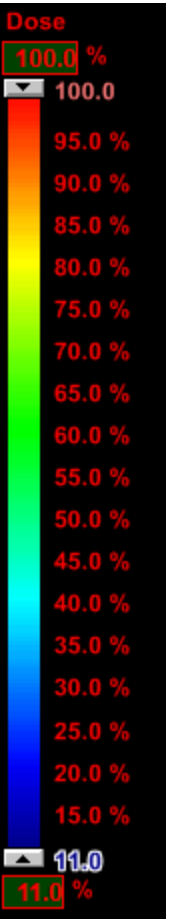

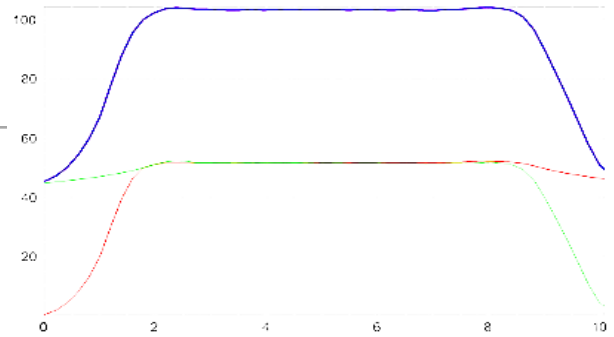

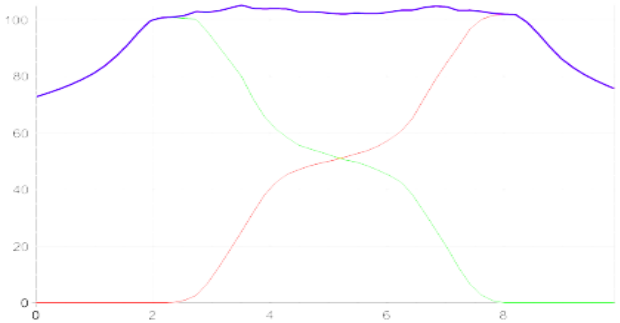

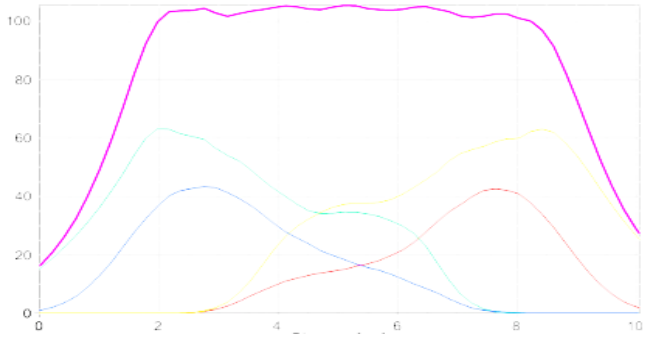

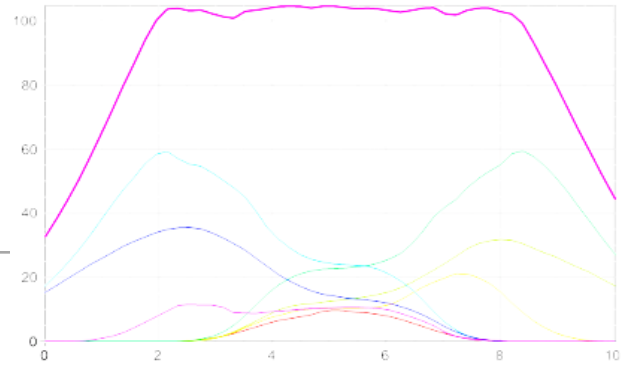

Dose – LET_d Comparison

Standard Full Target

2 Field Split Target

4 Field Split Target

7 Field Split Target

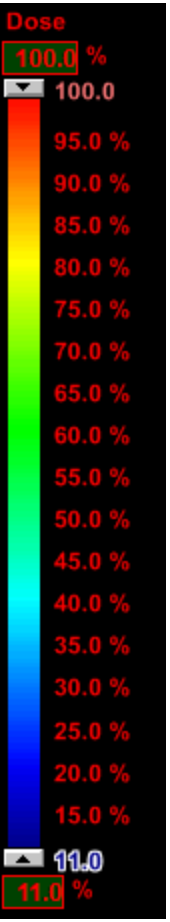

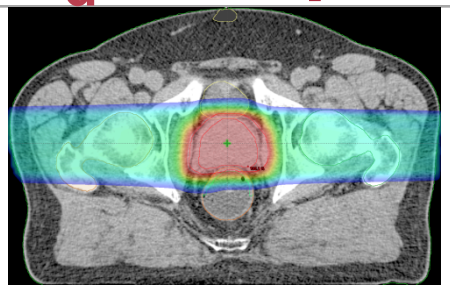

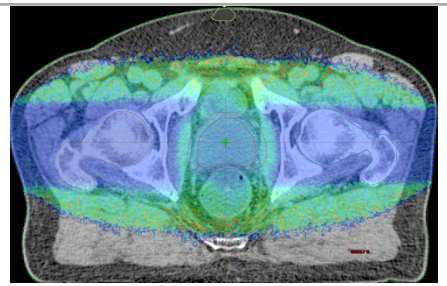

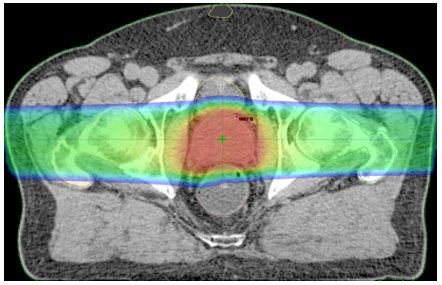

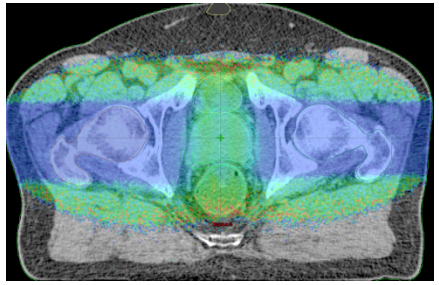

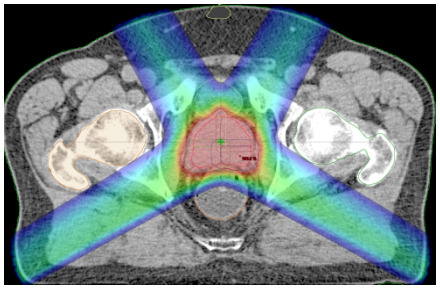

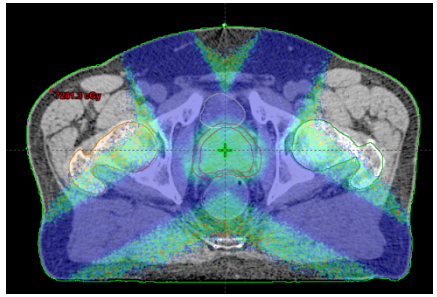

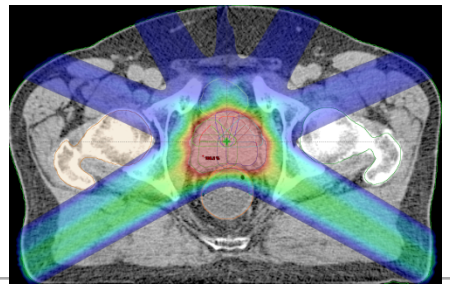

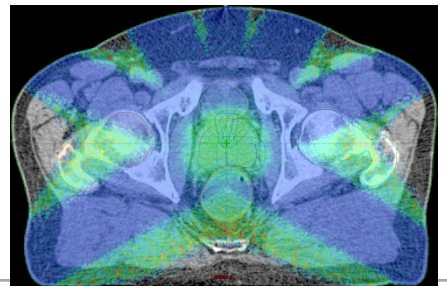

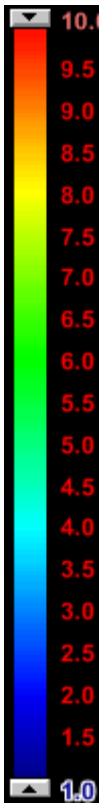

Perelman School of Medicine
University of Pennsylvania

Biophysical aspects of current proton treatment planning approaches

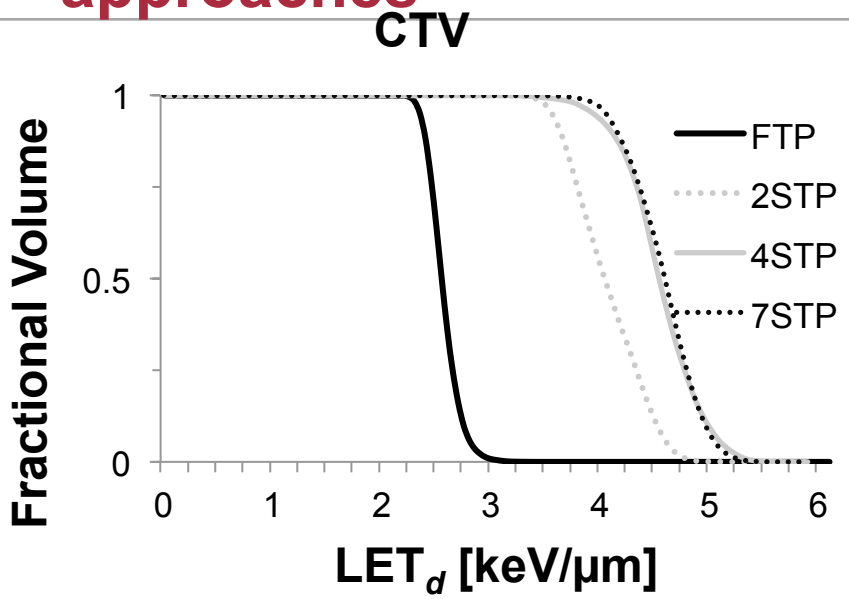

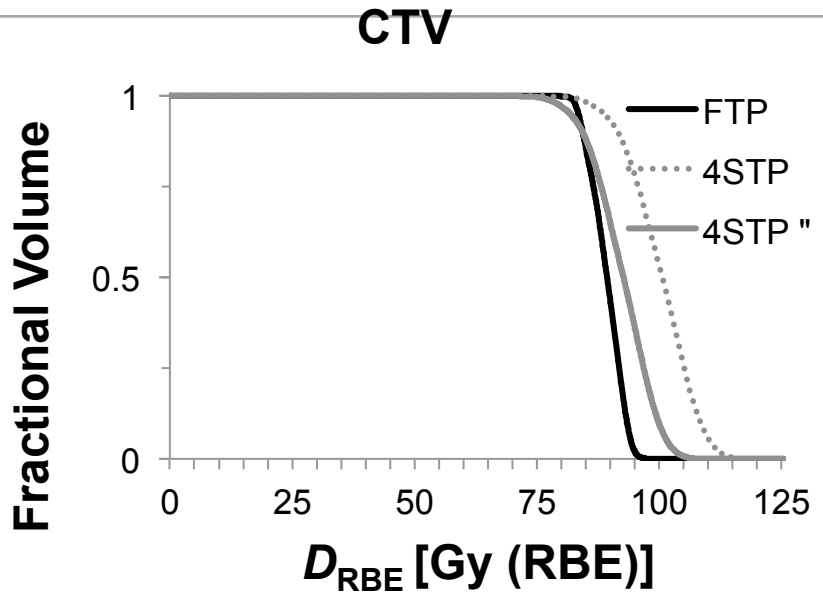

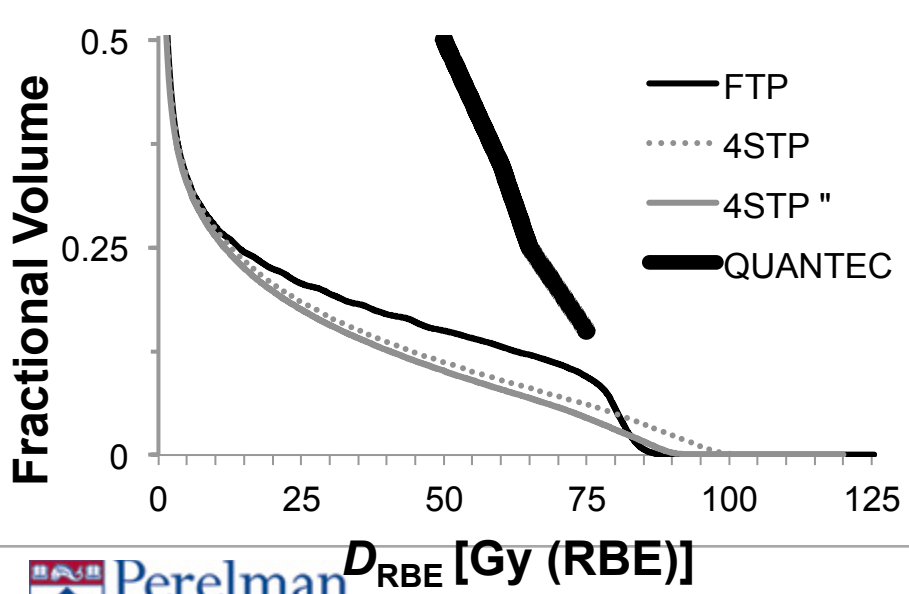

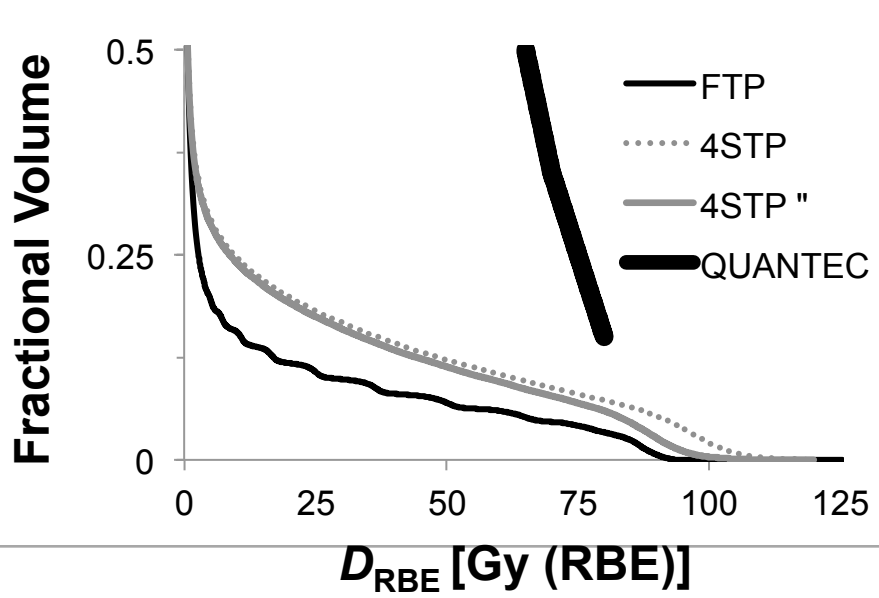

Biophysical aspects of current proton treatment planning approaches

Purpose: To propose a proton treatment planning method that trades fractional physical dose (d) for dose-averaged Linear Energy Transfer (LET_d) while keeping the radiobiological weighted dose D_{RBE} to the target the same.

Methods: The target is painted with LET_d by using 2, 4 and 7 fields aimed at the proximal segment of the target (split target planning, STP). As the LET_d within the target increases with the increasing number of fields, the physical dose per fraction decreases to maintain the D_{RBE} the same as the conventional treatment planning method using beams treating the full target (full target planning, FTP).

Results: The LET_d increased inside the target by 61% for 2STP, 72% for 4STP and 82% for 7STP, compared to FTP. This increase in LET_d led to a decrease of d with 0.16±0.01Gy for 2STP, 0.2±0.03Gy for 4STP and 0.21±0.01Gy for 7STP keeping the D_{RBE} constant to FTP.

Conclusions: LET_d painting offers a method to reduce prescribed dose at no cost for the biological effectiveness of the treatment.

2STP: 9% (1.8GyE)

4STP:11% (1.8GyE)

7STP:12% (1.8GyE)

Fager et al., 2014 (submitted)

What dose decrease percentage can we get if we go from discrete beams to…

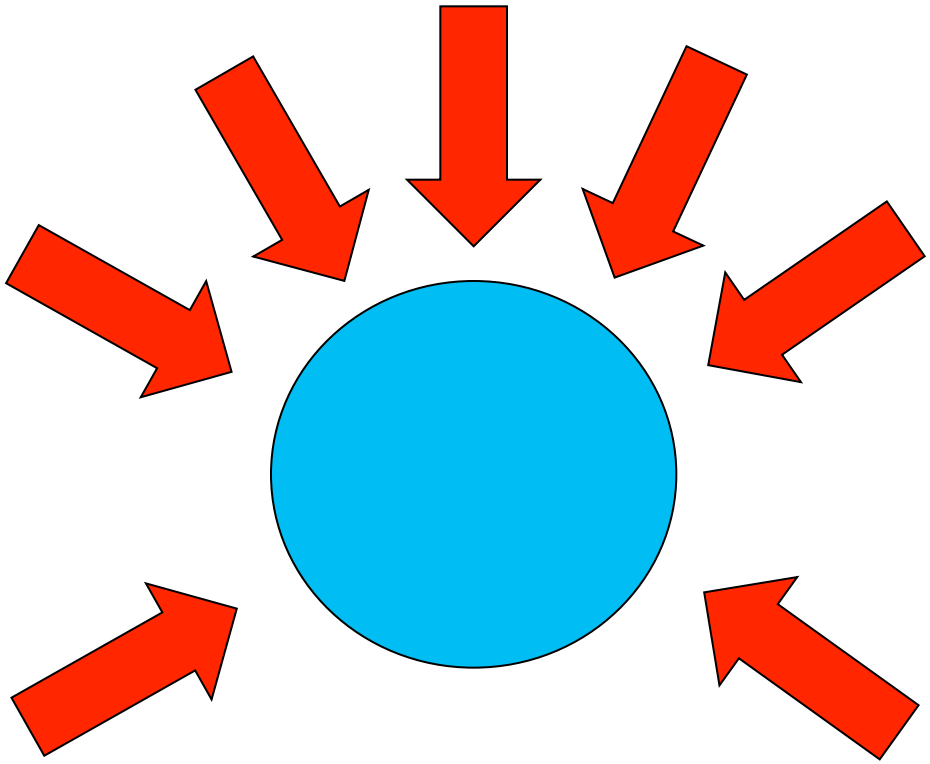

… continuous beam delivery

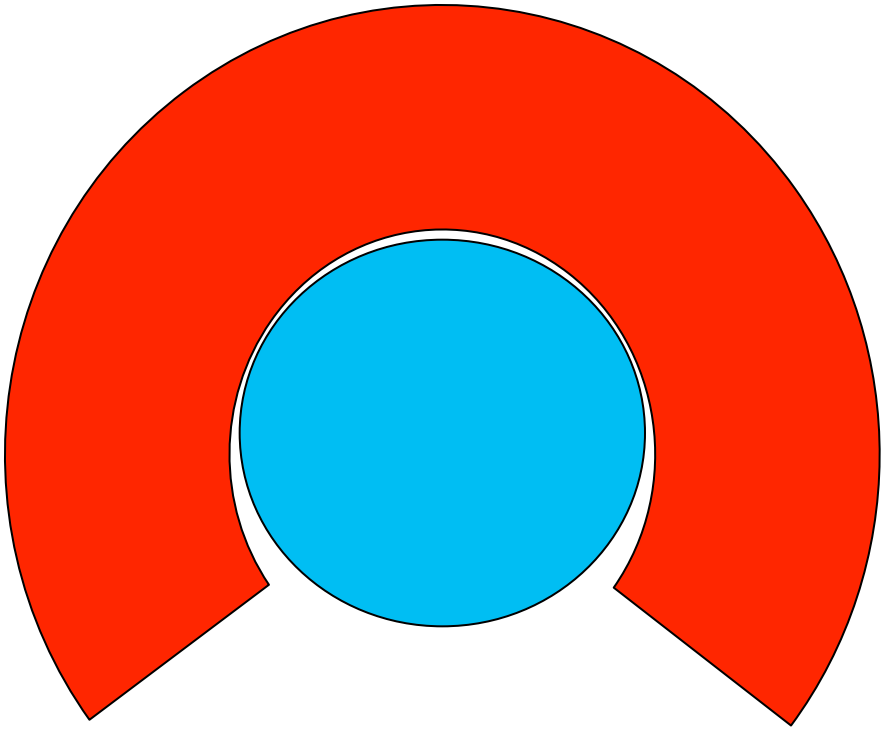

PROTON MODULATED ARC THERAPY (PMAT)

PMAT feasibility in PBS

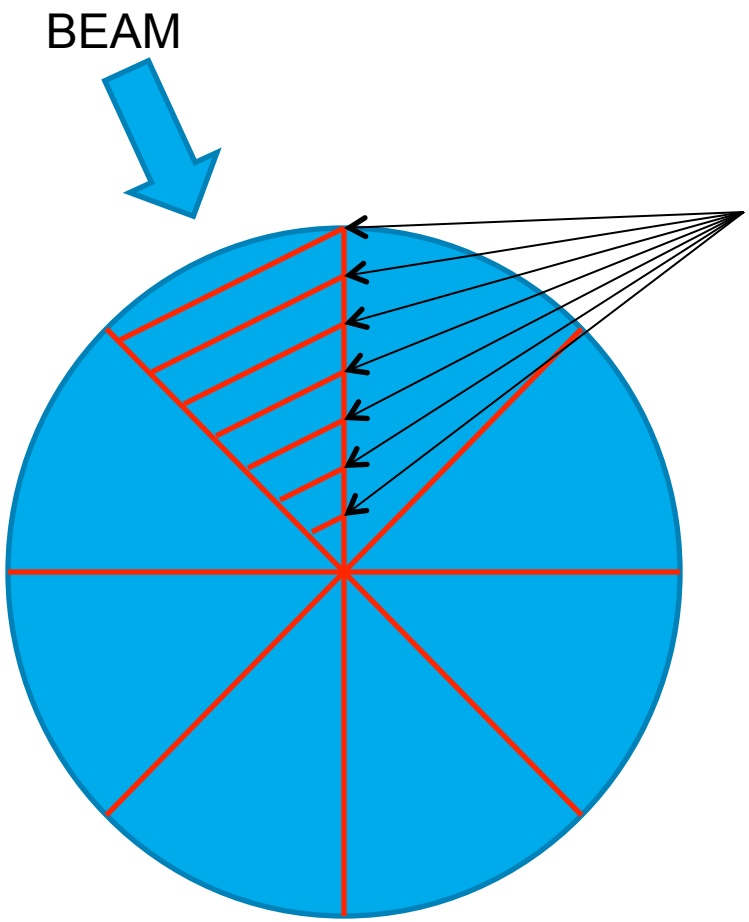

Multiple energy layers per angle

Gantry cannot rotate continuously

PMAT is not feasible in PBS mode

PMAT feasibility in PBS

But, what if… shut a mono-energetic beam

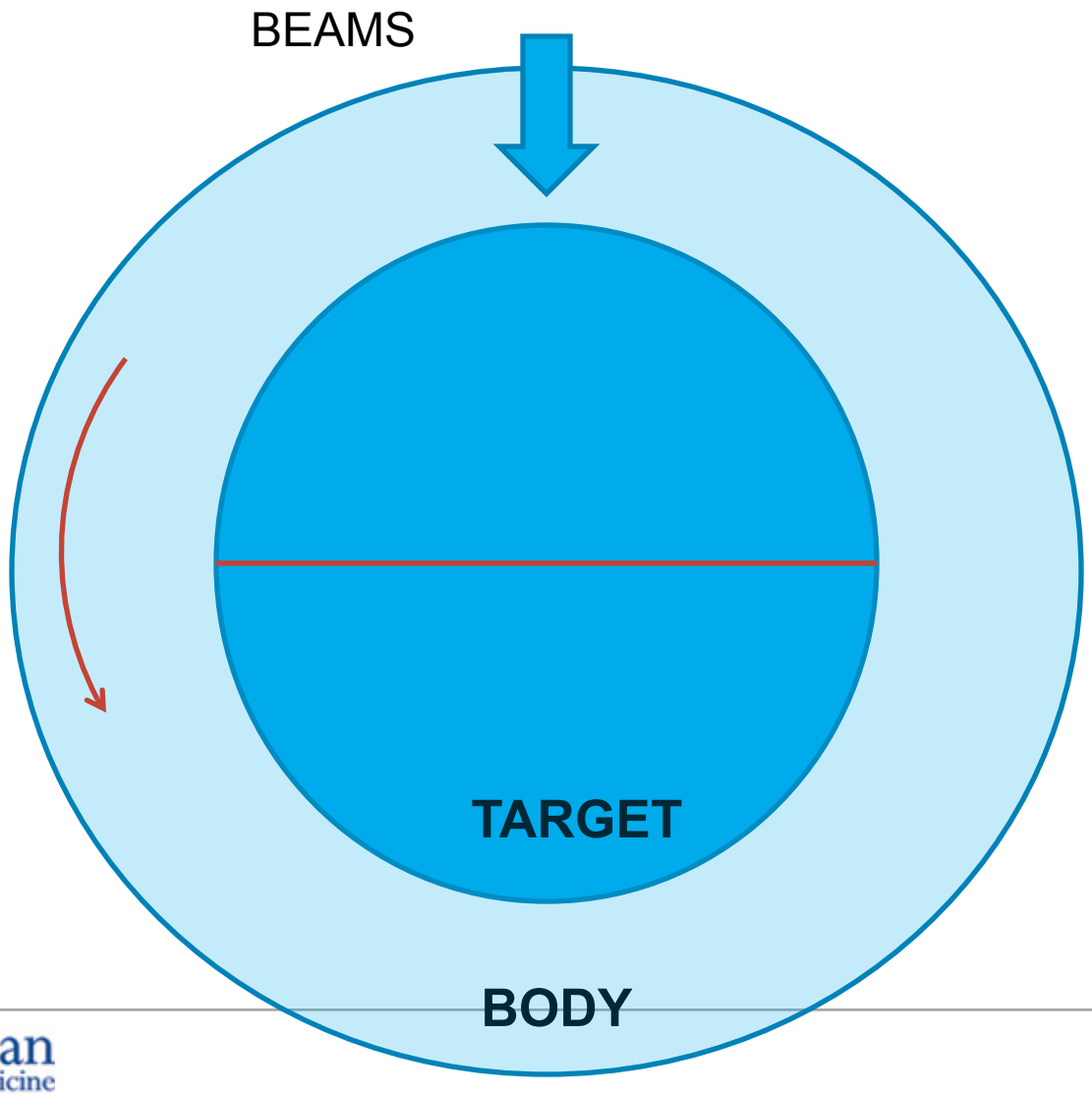

PMAT feasibility in PBS

… and let the gantry rotation take care of the target dose painting

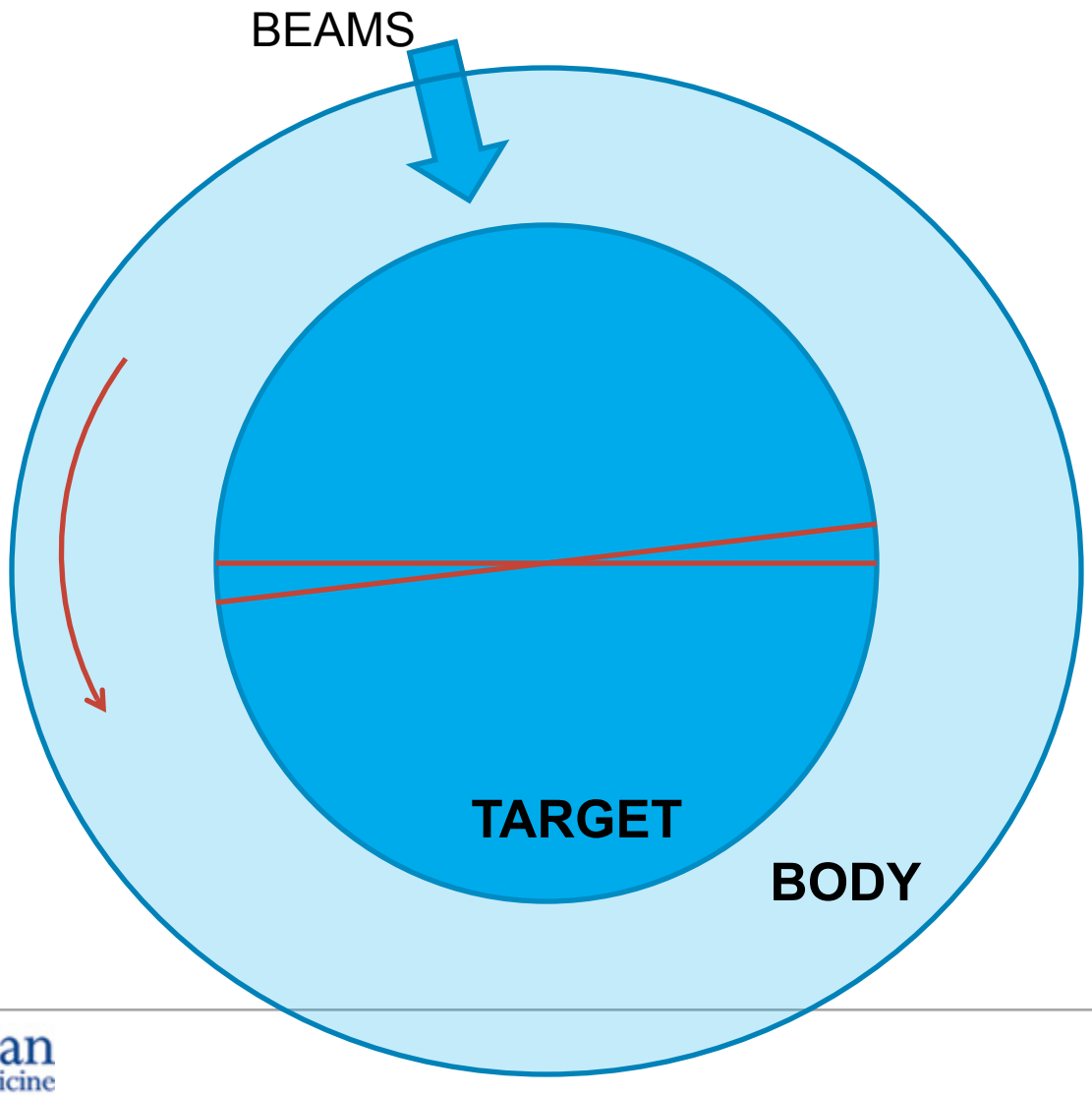

PMAT feasibility in PBS

… and let the gantry rotation take care of the target dose painting

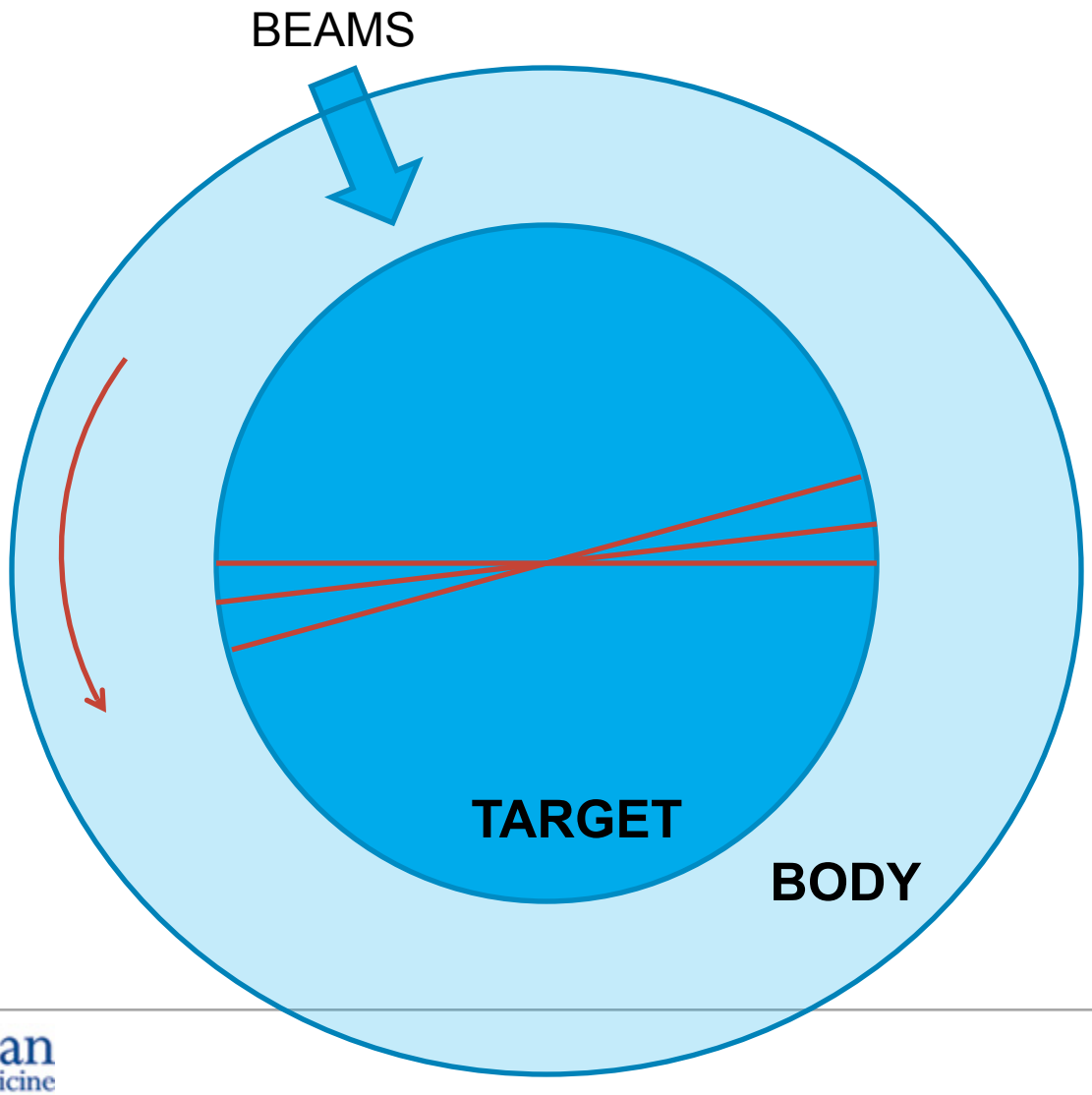

PMAT feasibility in PBS

… and let the gantry rotation take care of the target dose painting

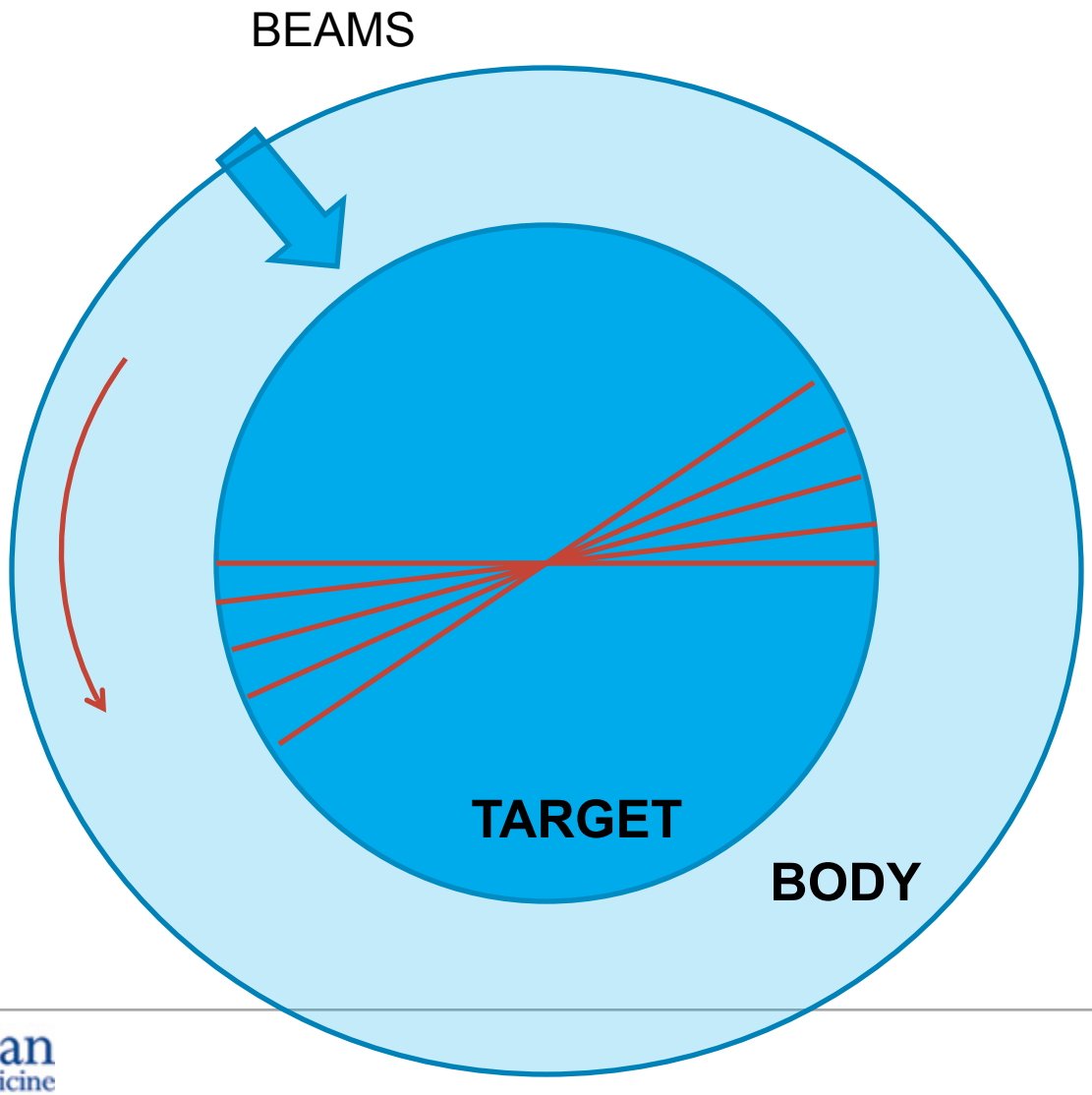

PMAT feasibility in PBS

… and let the gantry rotation take care of the target dose painting

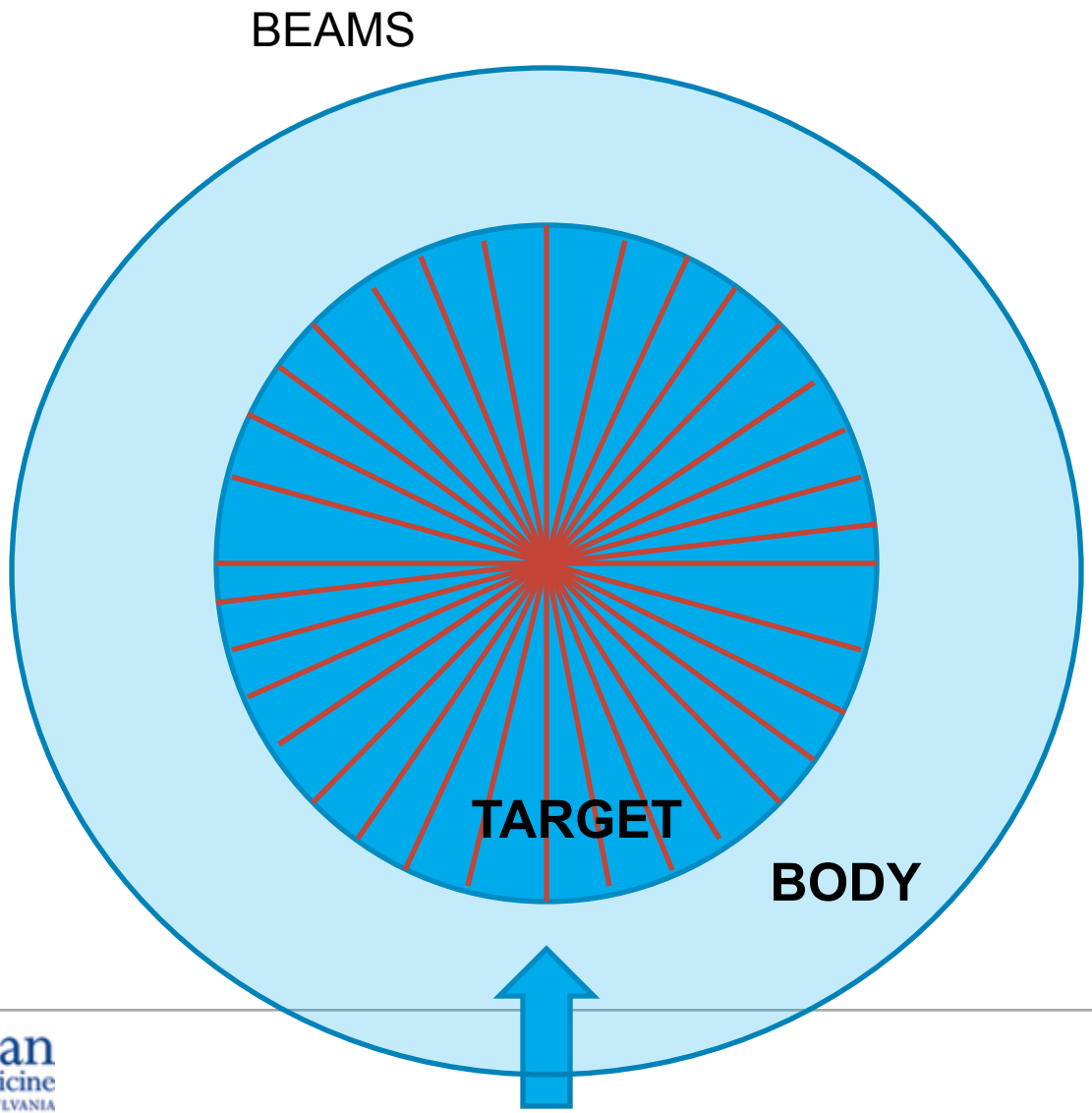

PMAT feasibility in PBS

But one single energy will not be able to cover targets within irregular/inhomogeneous body shapes

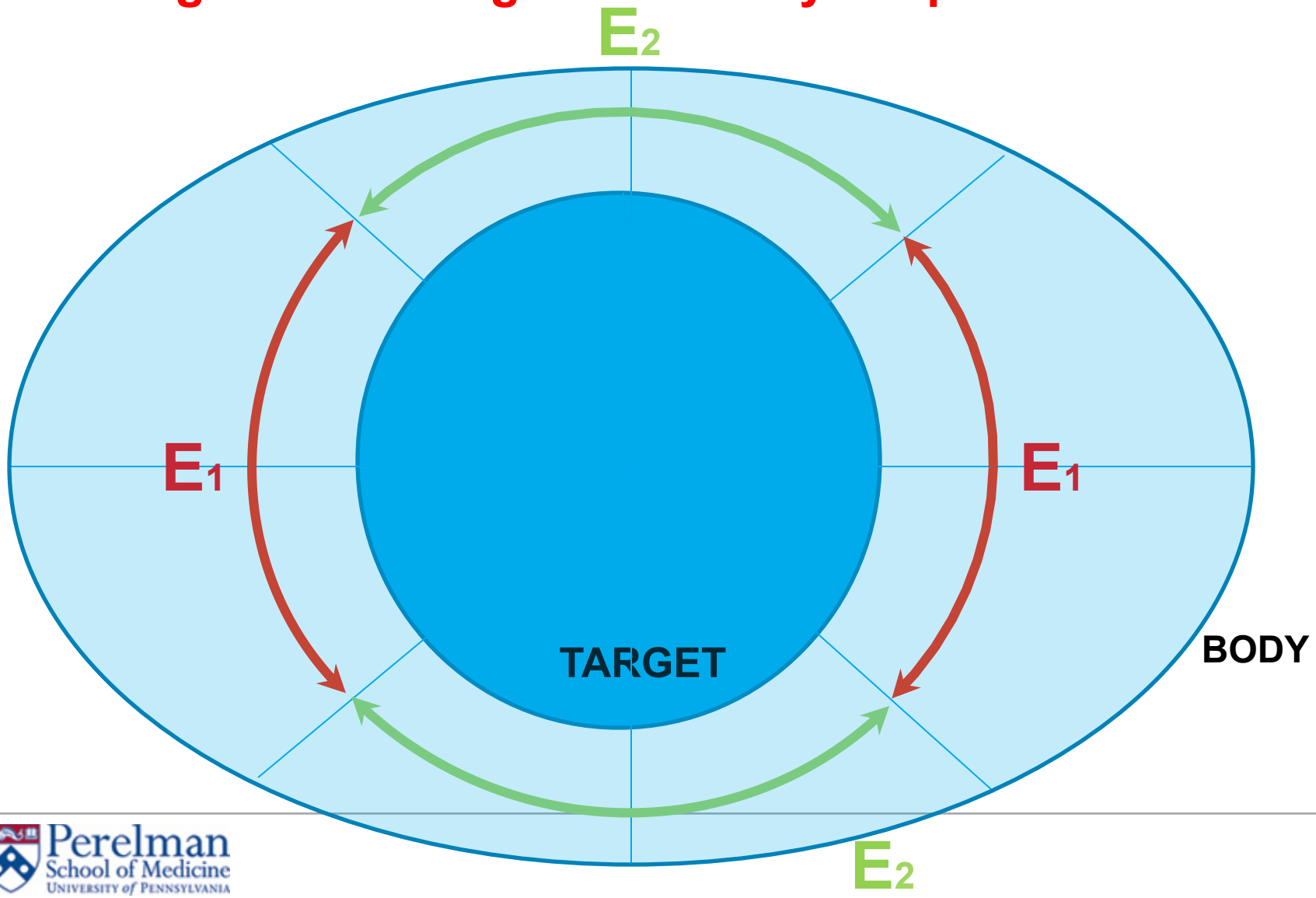

PMAT feasibility in PBS

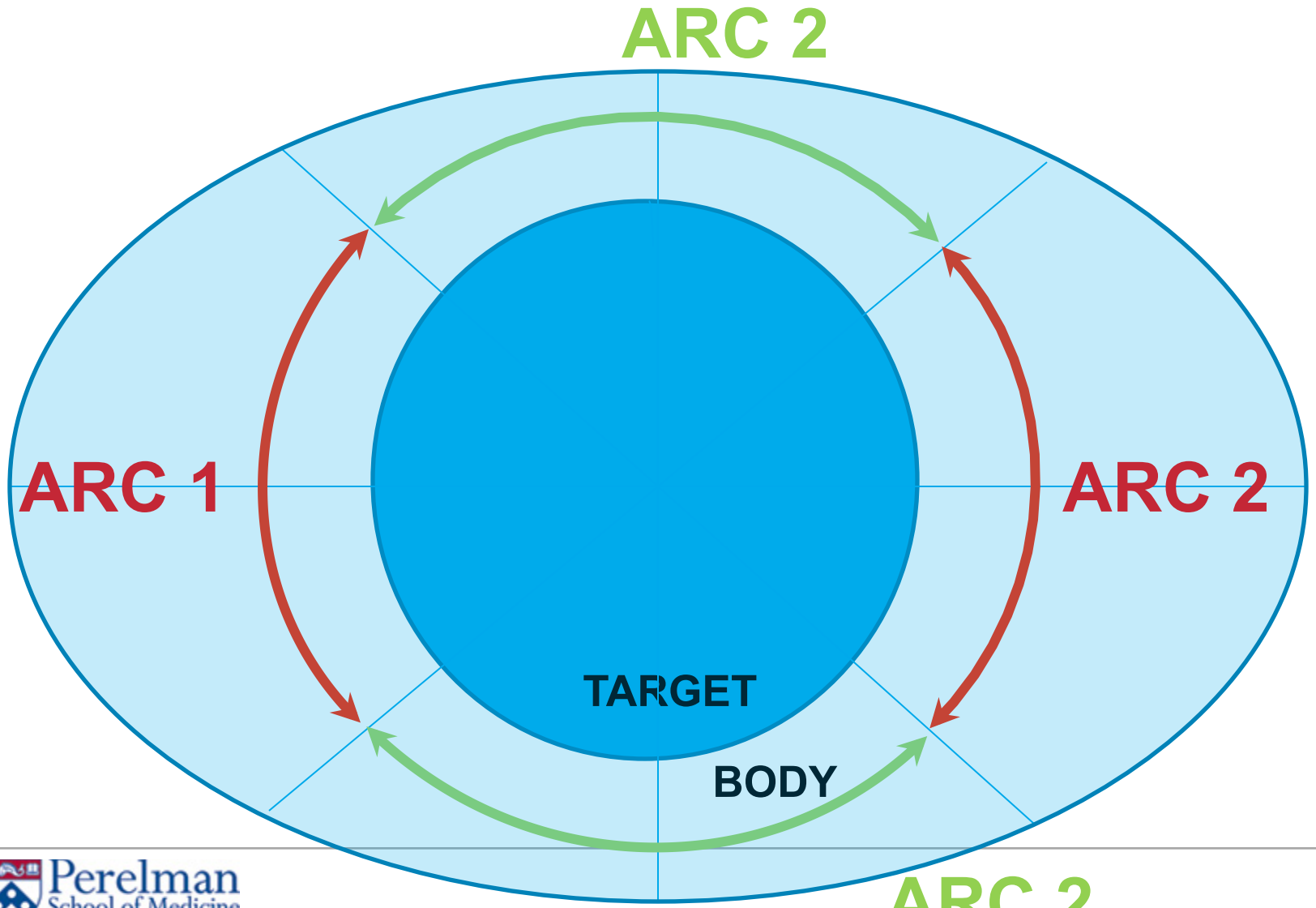

PMAT vs PBS treatment of Brain tumor

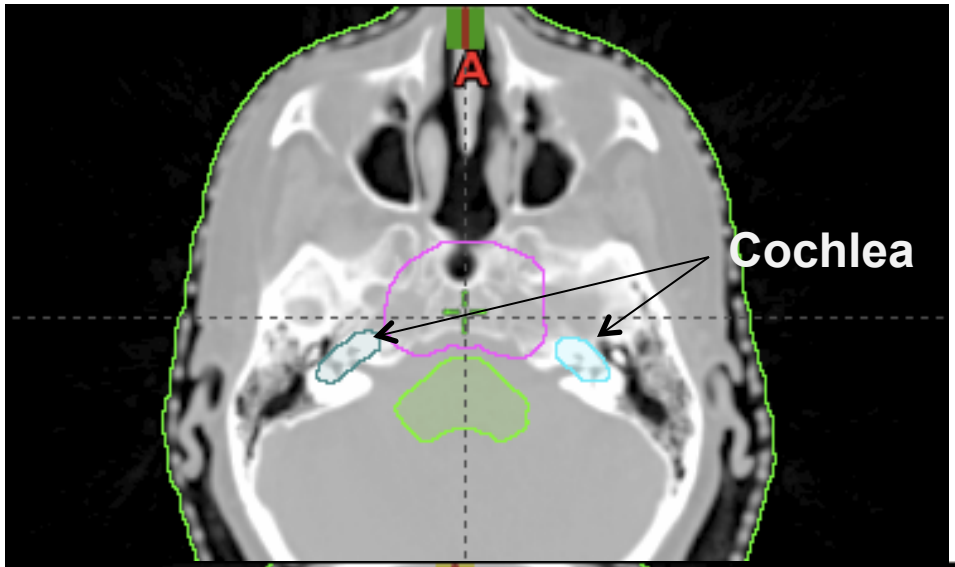

7920cGy / 44 fraction

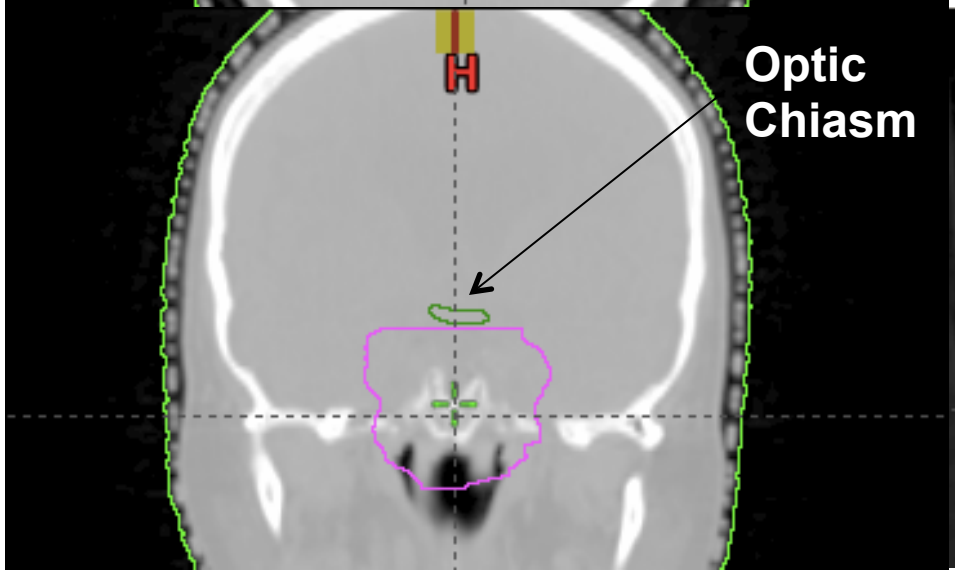

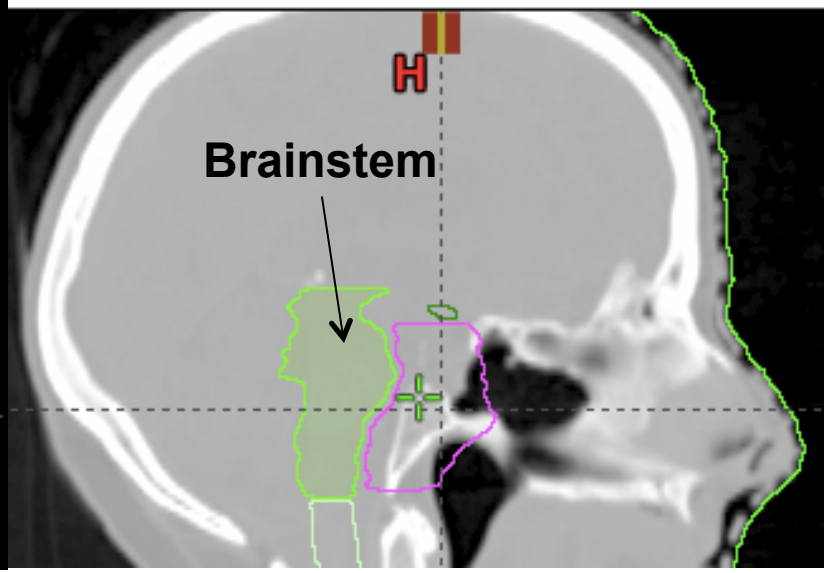

PMAT in Brain tumor

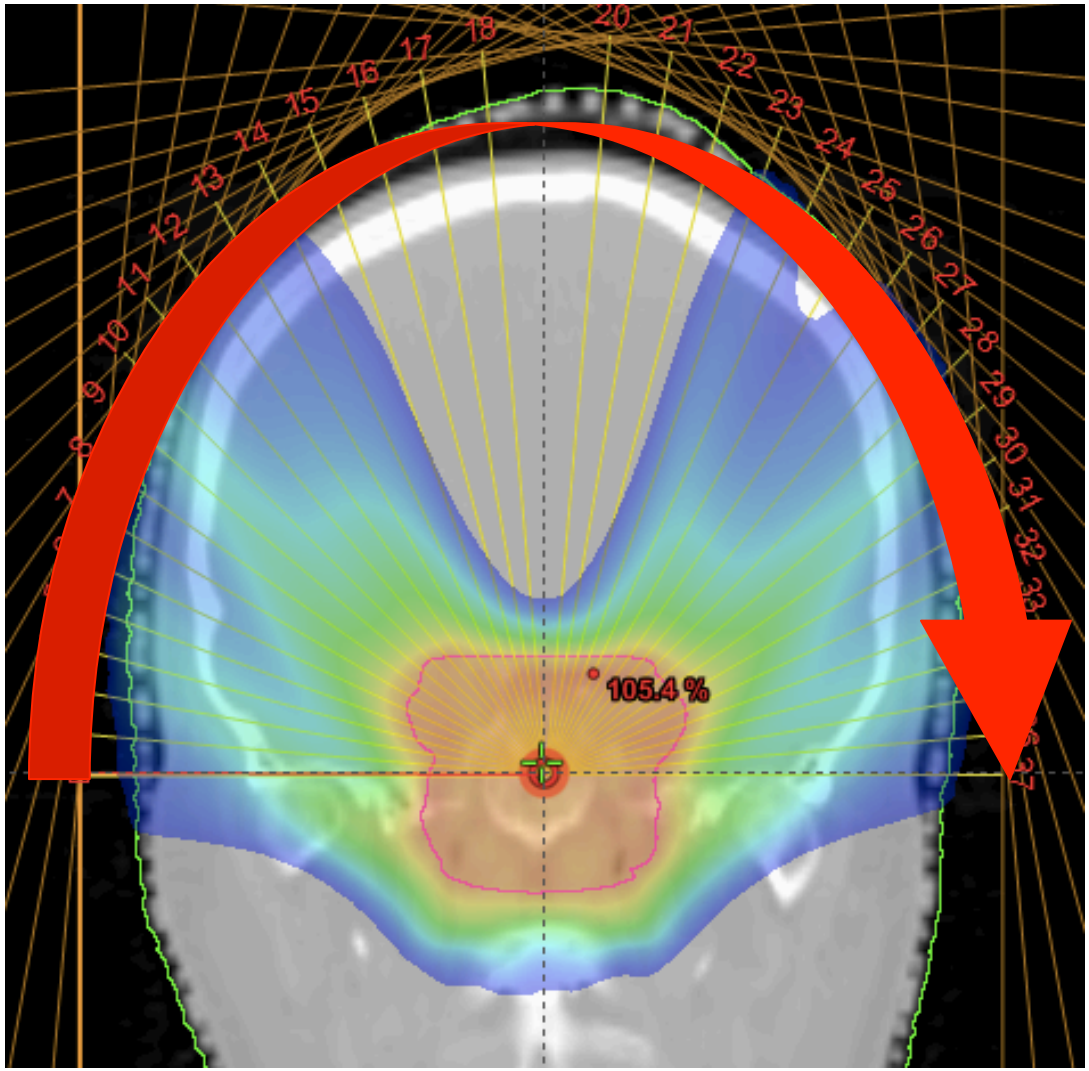

ARC 1 (E_1=113.2MeV)

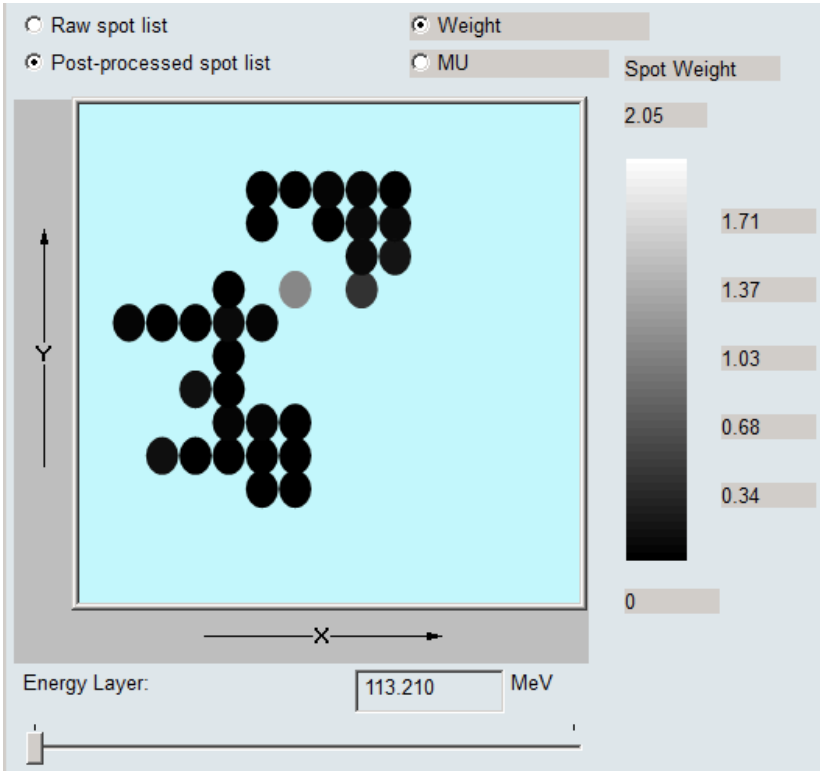

PMAT in Brain tumor

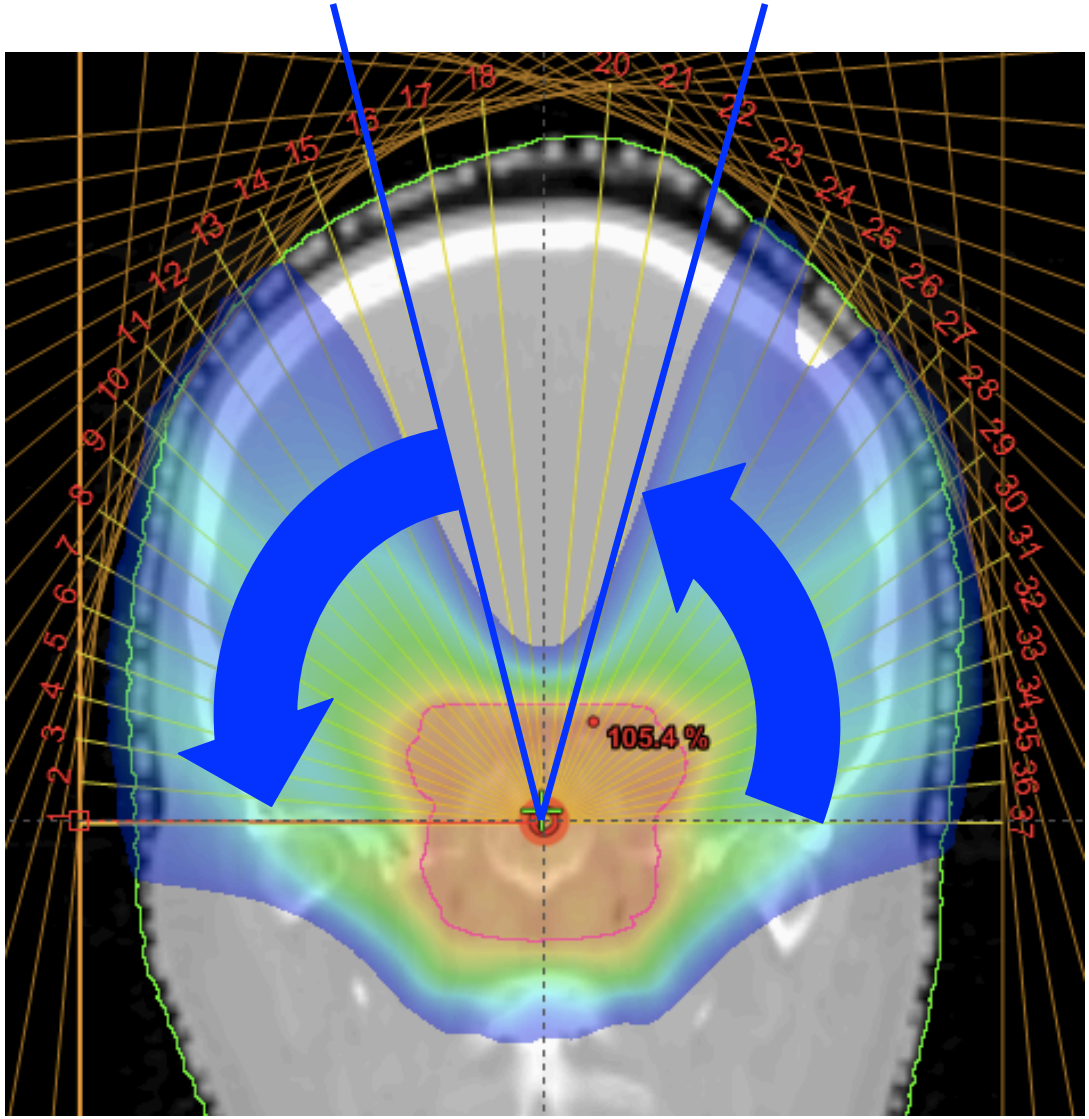

ARC 2 (E_1=110.2MeV)

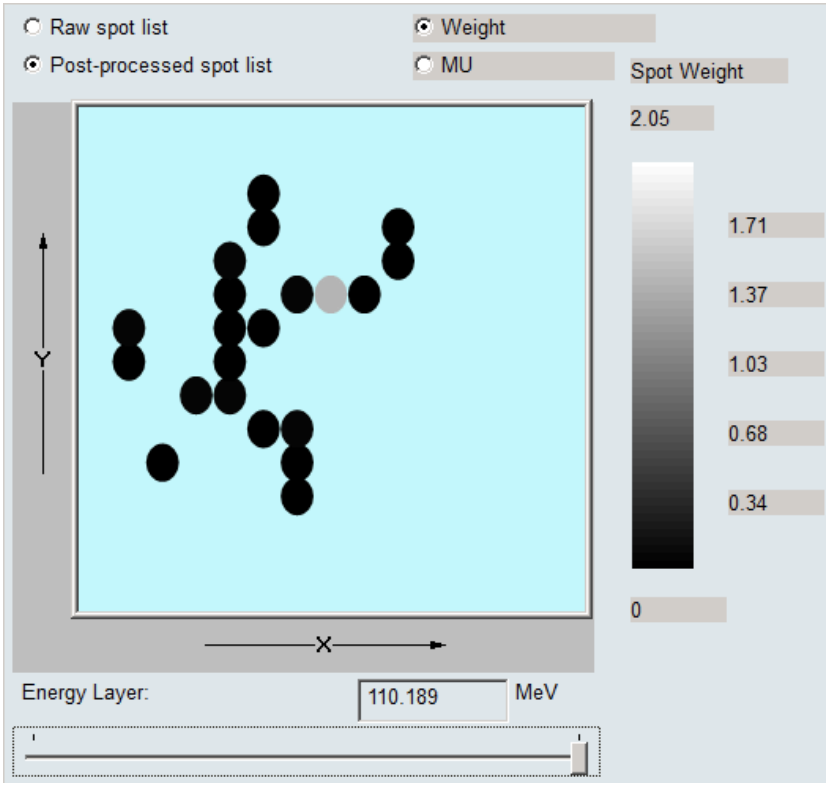

PMAT-DOSE

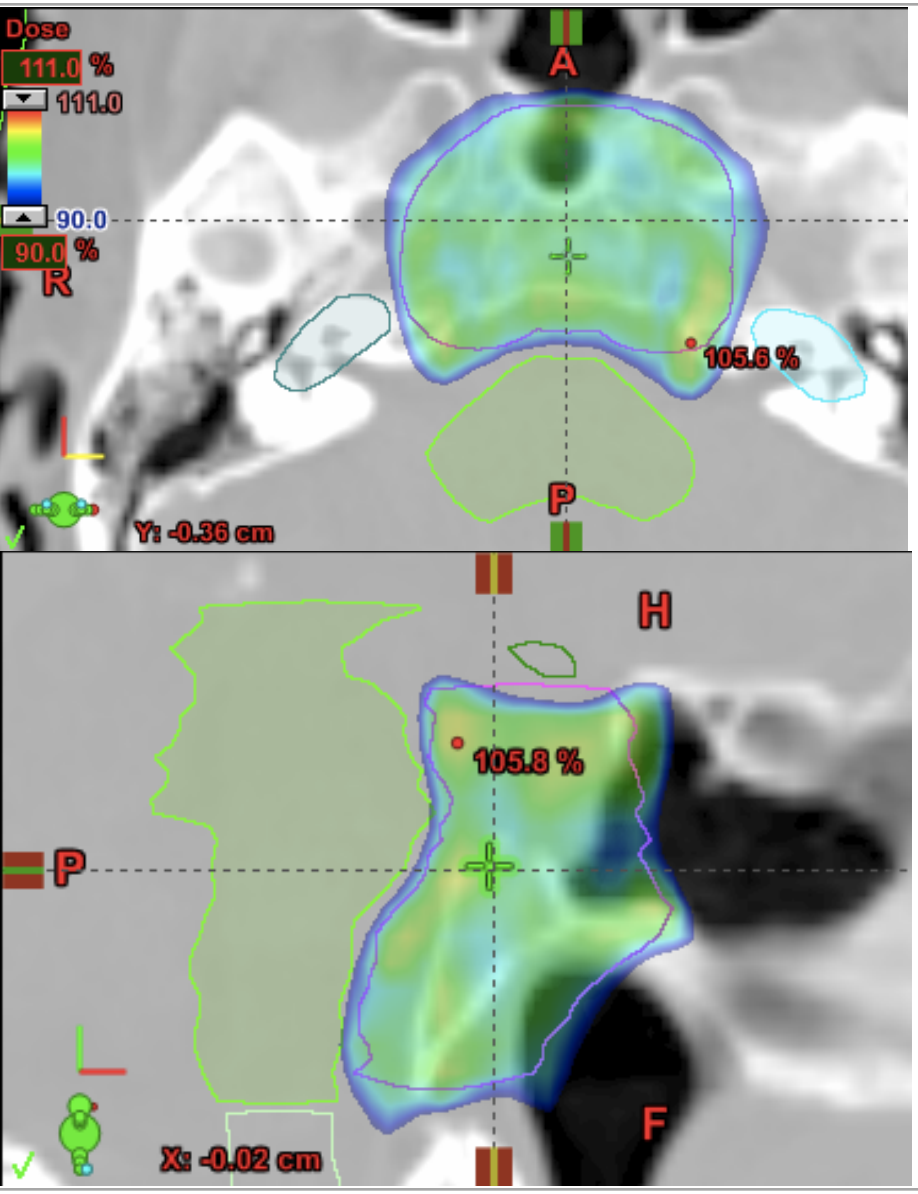

PBS-DOSE

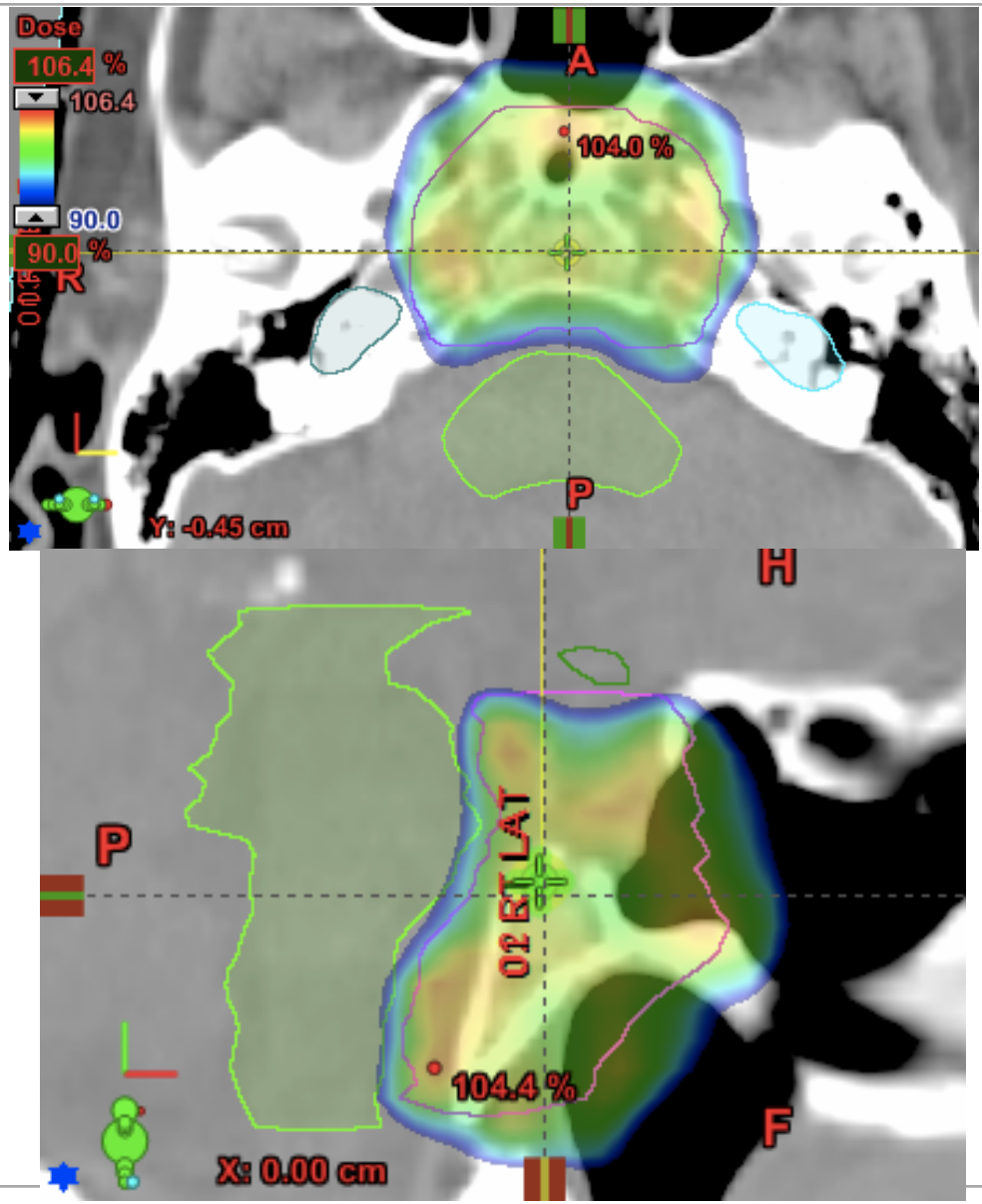

Perelman School of Medicine
University of Pennsylvania

PMAT vs PBS: DVH

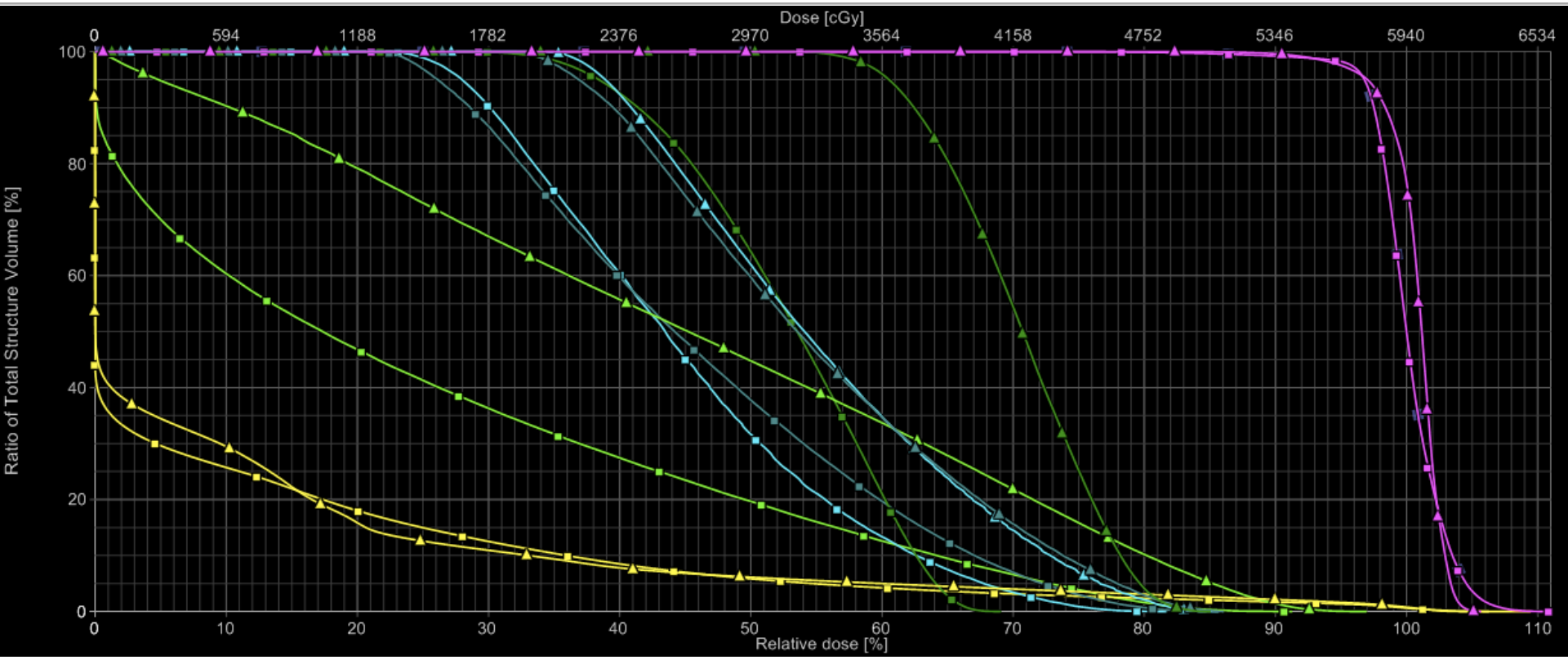

BRAINSTEM
Brain
COCHLEA_L
COCHLEA_R
OPTIC CHIASM
CTV 59.4 rev

(R)37_Min_950
INI_PBS

PMAT-LET

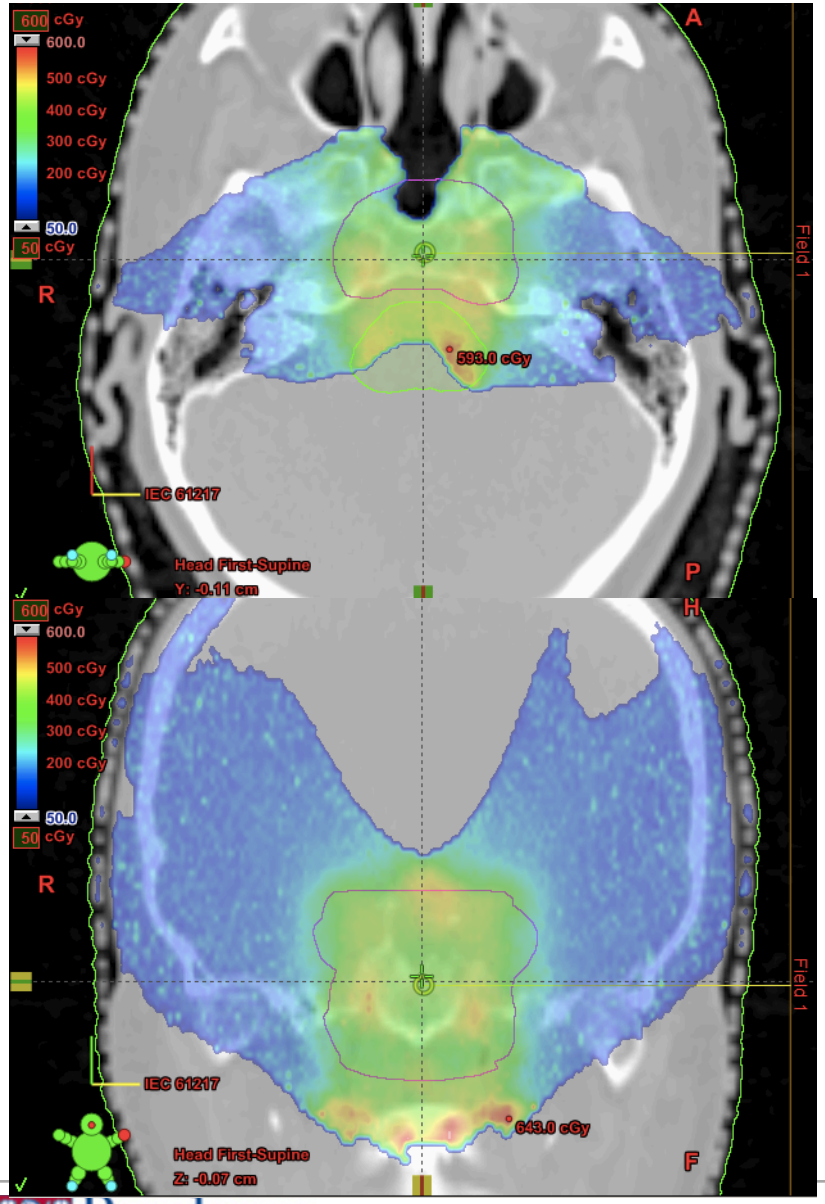

PBS-LET

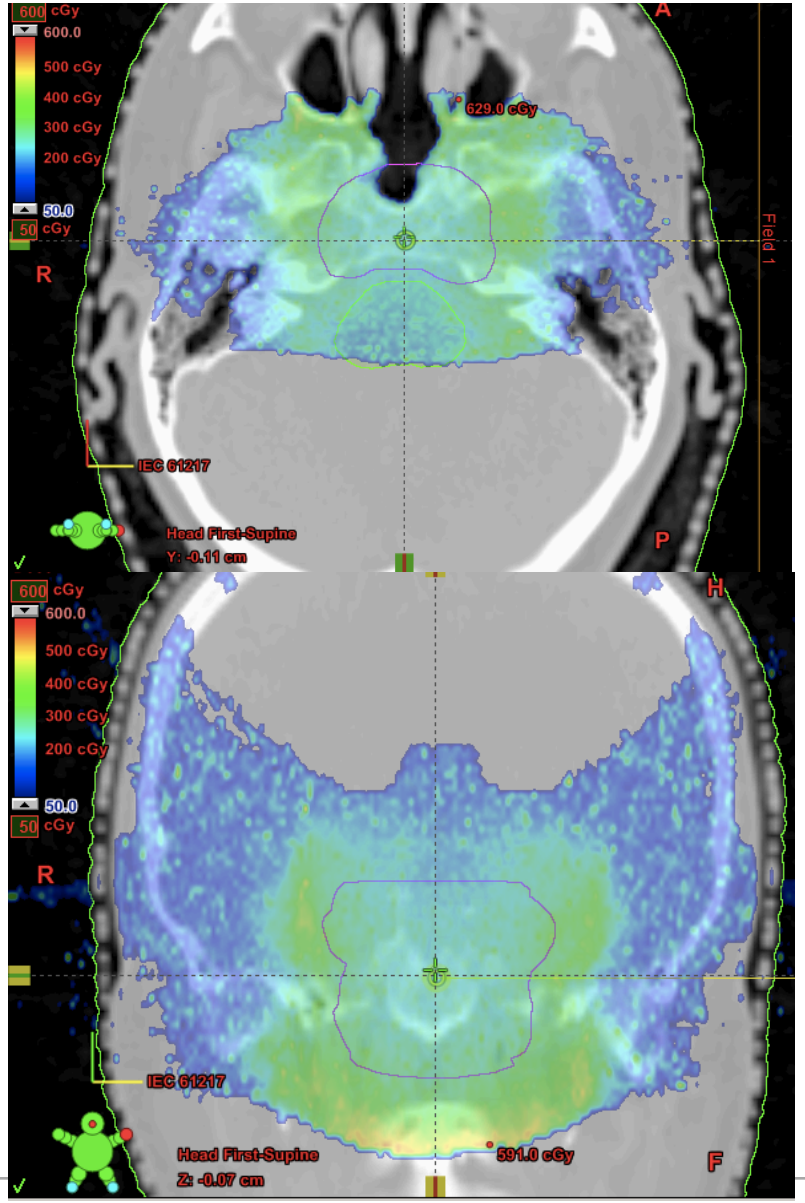

Perelman School of Medicine
University of Pennsylvania

PMAT vs PBS: LET-VH

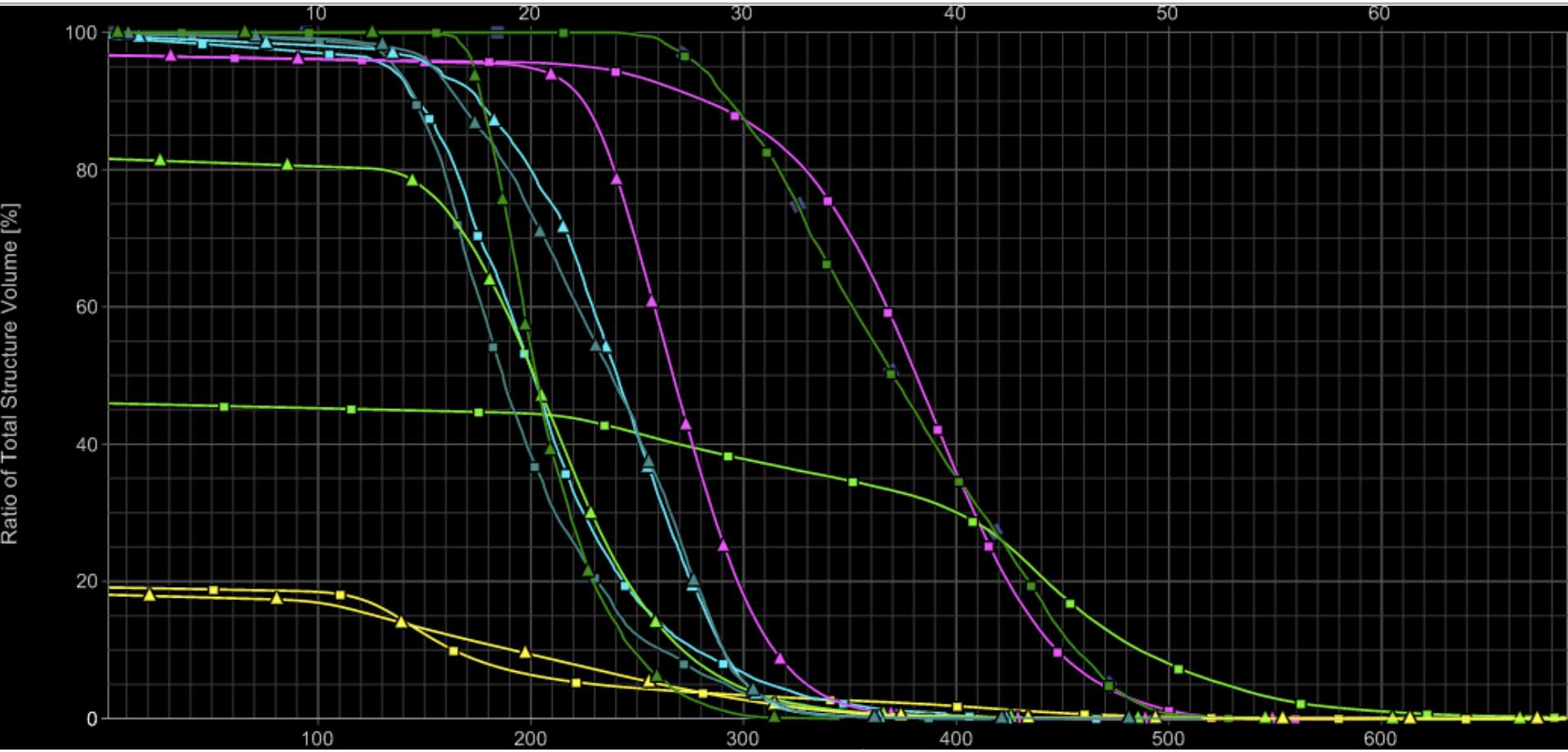

Inverse TPS prototype based on MLC

Work done by: Daniel Sanchez-Parcerisa – University of Pennsylvania

Example: DS-PAT in a cylindrical phantom

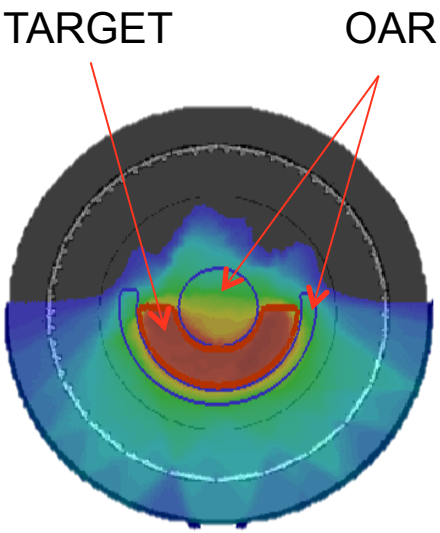

PHANTOM example
13 fields, every 15 deg

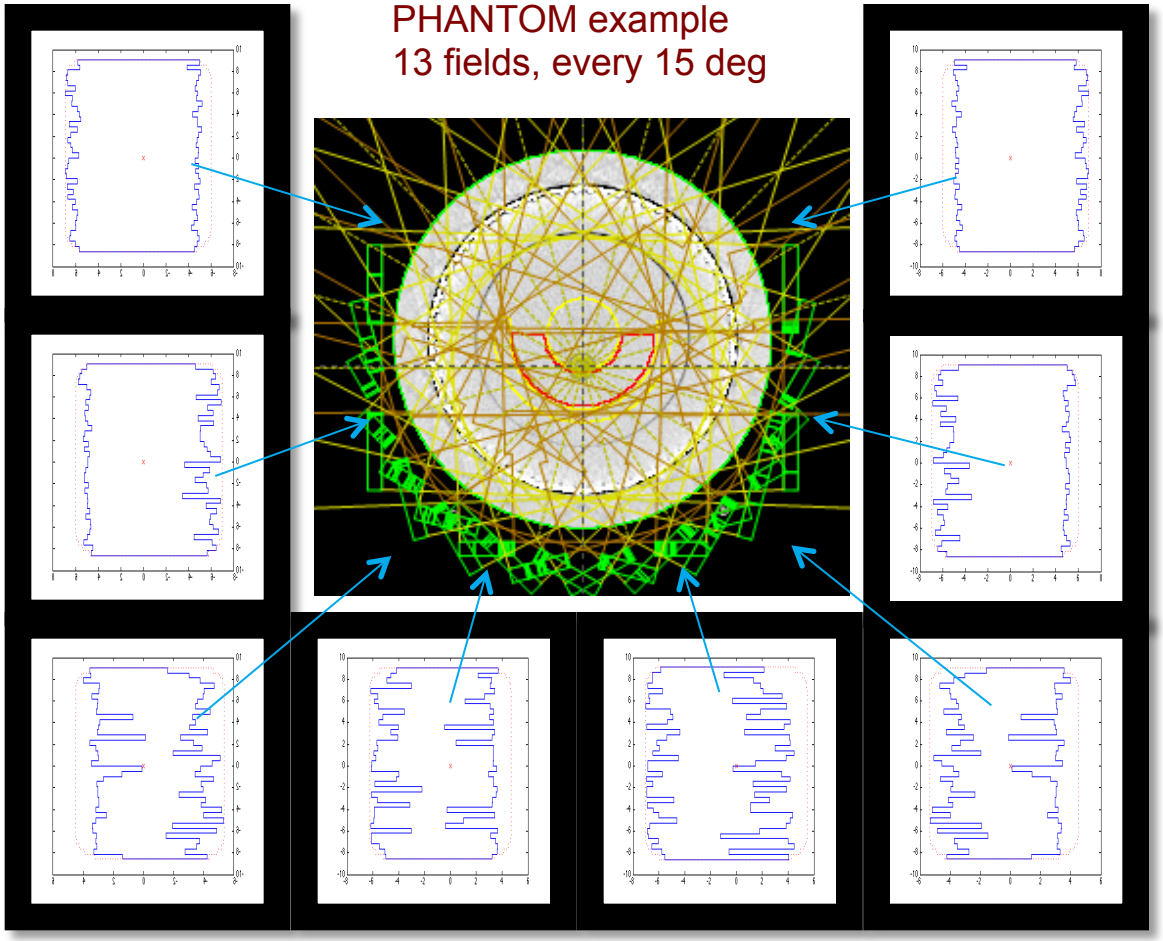

Poster: SU-E-T-214

Sanchez-Parcerisa et al. (2014)

Elements of Radiobiological Optimization

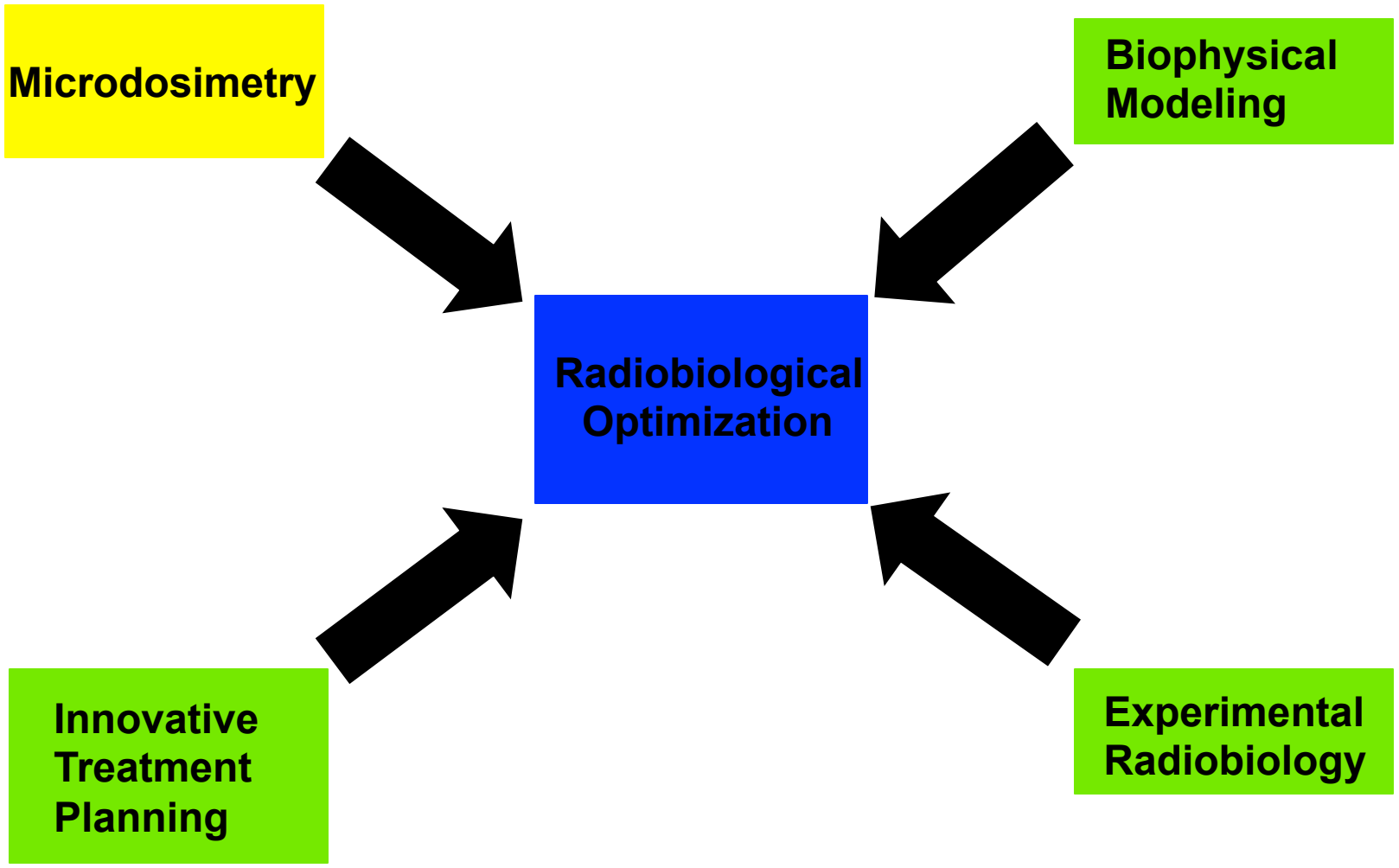

Correct calculations of LET

Work done by: M. A. Cortés-Giraldo – University of Seville (Spain)

- To analyze the difference in the LET_d values predicted by the different definitions presented in the literature used for these calculations.
- To prove the correct definition based on the LET_d obtained as the limiting value of a microdosimetric experiment.

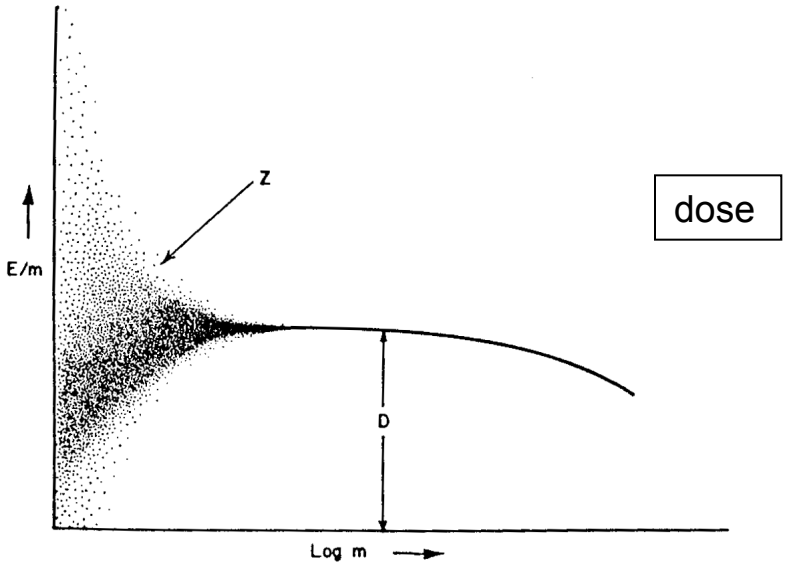

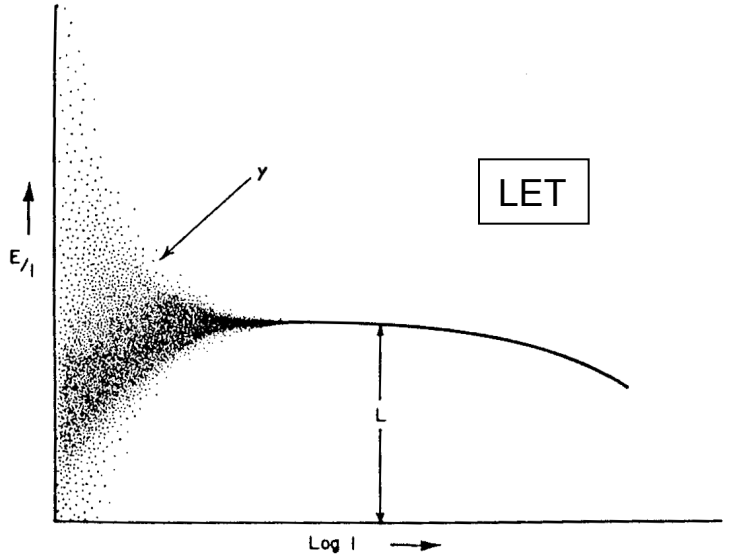

Difference between calculation methods

Monte Carlo calculation of LET_d:

$$\overline{L}_{\mathrm{d}}(\vec{x}) = \frac{1}{\rho} \frac{\sum_{\mathrm{evt}} \left(\frac{\mathrm{d}E}{\mathrm{d}x}\right) \mathrm{d}E}{\sum_{\mathrm{evt}} \mathrm{d}E}$$

Consider a certain voxel irradiated by *N* events (primary particles):

- T_n tracks transported along the voxel at event ***n***.
- Each track ***t*** makes S_{tn} steps within the voxel.

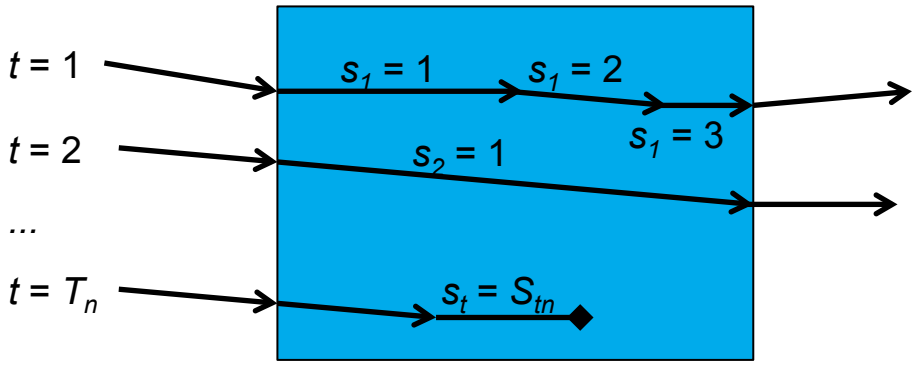

- *n* = event index
- *t* = track index
- *s* = step index

Difference between calculation methods

- ω = track weight
- ε = energy deposited per step(*)
- l = step length

$$\bar{L}_{\mathrm{d}}(\vec{x}) = \frac{1}{\rho} \frac{\sum_{\mathrm{evt}} \left(\frac{\mathrm{d}E}{\mathrm{d}x}\right) \mathrm{d}E}{\sum_{\mathrm{evt}} \mathrm{d}E}$$

Cortés-Giraldo et al. (2014)

Method A

$$\bar{L}_{\mathrm{d}} = \frac{1}{\rho} \frac{\sum_{n=1}^{N} \sum_{s=1}^{S_n} \omega_n \frac{\varepsilon_{sn}^2}{l_{sn}}}{\sum_{n=1}^{N} \sum_{s=1}^{S_n} \omega_n \varepsilon_{sn}}$$

d*E*/d*L* computed step by step

Method B

$$\bar{L}_{\mathrm{d}} = \frac{1}{\rho} \frac{\sum_{n=1}^{N} \left[\omega_n \frac{\left(\sum_{s=1}^{S_n} \varepsilon_{sn} \right)^2}{\sum_{s=1}^{S_n} l_{sn}} \right]}{\sum_{n=1}^{N} \left[\omega_n \sum_{s=1}^{S_n} \varepsilon_{sn} \right]}$$

d*E*/d*L* computed along the voxel

Method C

$$\bar{L}_{\mathrm{d}} = \frac{1}{\rho} \frac{\sum_{n=1}^{N} \sum_{s=1}^{S_n} \omega_n L_{sn} \varepsilon_{sn}}{\sum_{n=1}^{N} \sum_{s=1}^{S_n} \omega_n \varepsilon_{sn}}$$

L_{sn} obtained from ICRU 49 stopping power tables for particle Residual range

(*) Kinetic energy of secondary electrons included in ε (unrestricted LET)

Macro-dosimetric calculations (LET)

Dose and LET_d simulation with Geant4 (v9.6.2)

Geometry

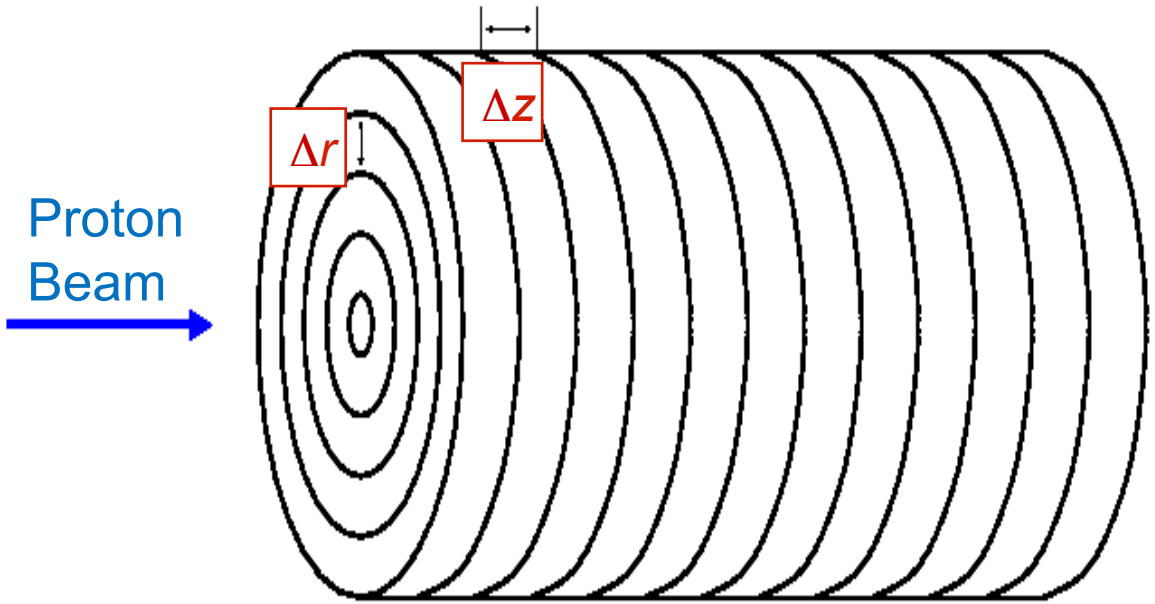

- Water tank – cylindrical symmetry
- Δz value from 0.2 – 2.0 mm
- Δr = 2.0 mm
- Dedicated scorers for LET_d

Physics

- StandardEM_option3
- QGSP_BIC_HP
- Prod. cut = 0.05 mm

Proton Beam

- 160 MeV beamlet
- Broad beam for SOBP

Macro- vs Micro-dosimetric comparison

According to Kellerer (1985)

$$\bar{L}_{\mathrm{d}} = \frac{8}{9}\left(\bar{y}_{\mathrm{D}} - \frac{3\delta_2}{2d}\right)$$

Where:

- δ_2 represents the weighted average of the energy loss per collision, ε_c, of the traversing charged particle.
- *d* represents the site diameter

Results – LET_d calculations

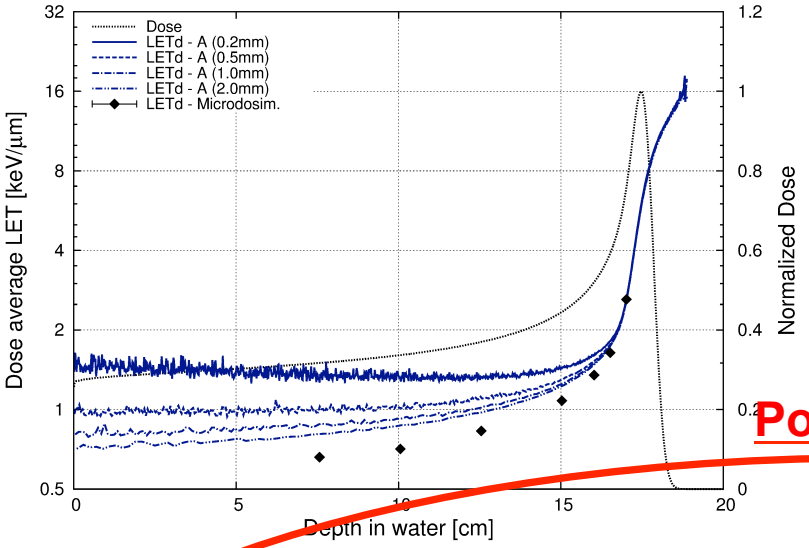

protons @ 160 MeV

Method A (step-by-step)
Method B (along voxel)
Method C: dE/dx tables

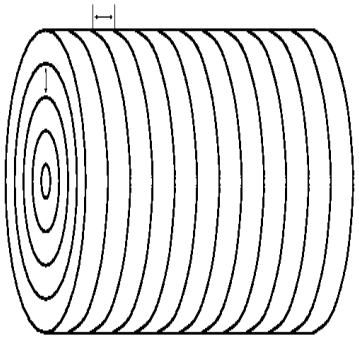

Poster: SU-E-T-78

Integrated over 5mm around central axis

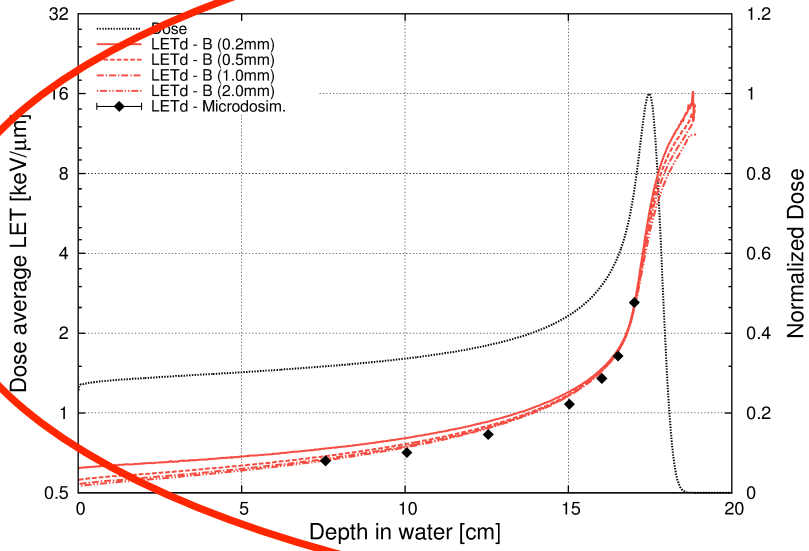

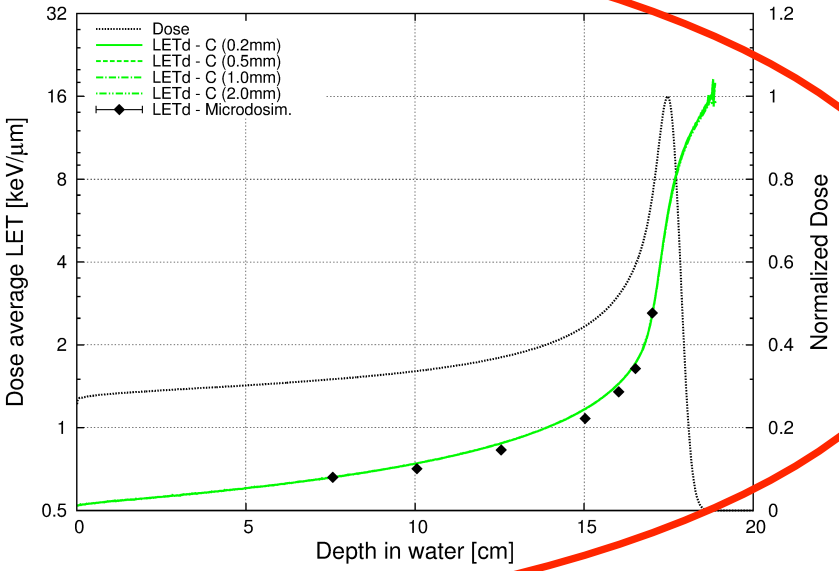

Perelman School of Medicine
University of Pennsylvania

Results – LET_d calculations

Differences – entrance region

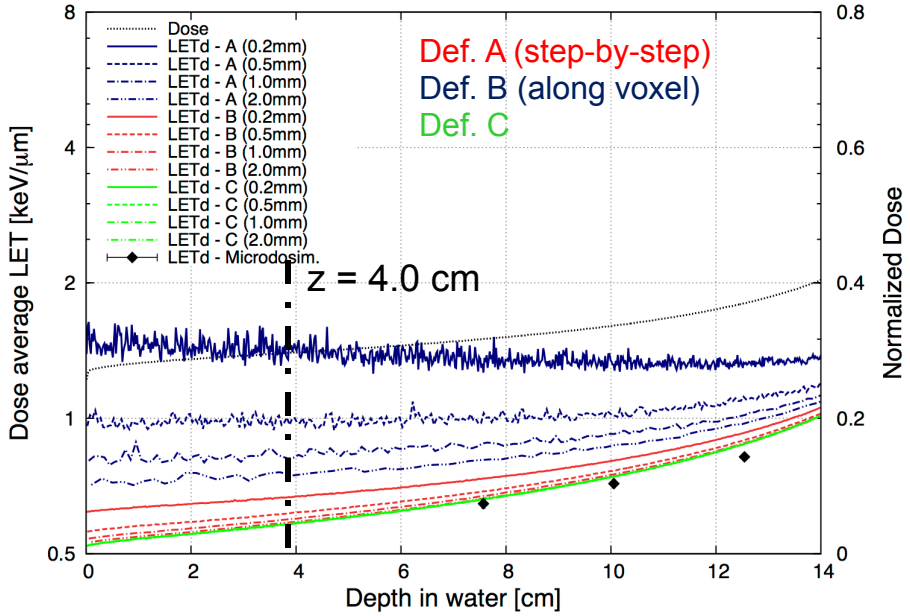

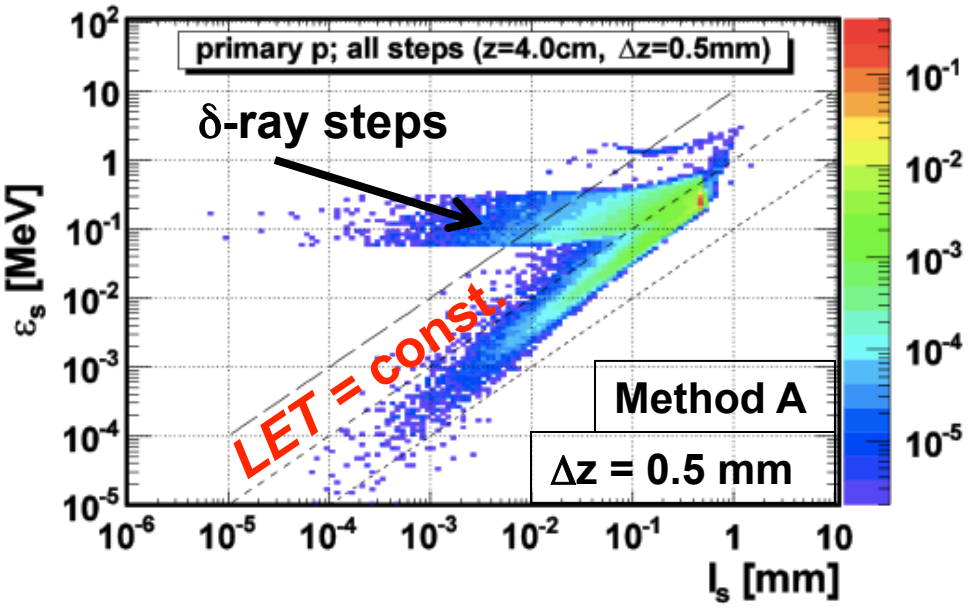

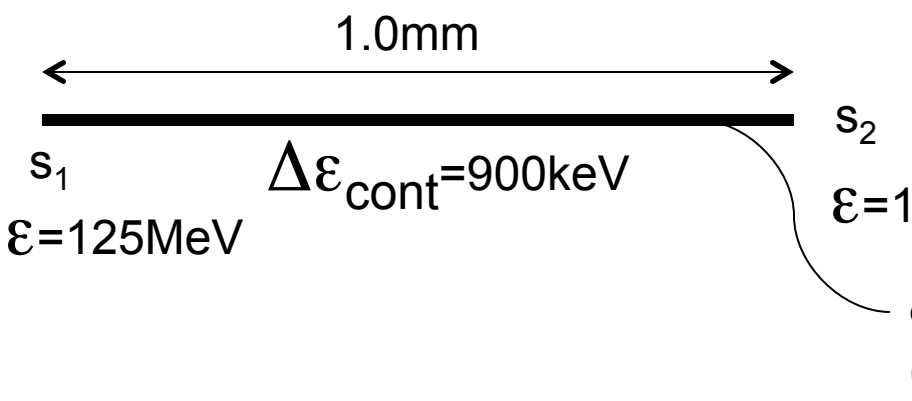

$$L \approx \frac{0.900 + 0.100}{1.0}\frac{MeV}{mm} = 1\frac{MeV}{mm}$$

Results – LET_d calculations

Differences – entrance region

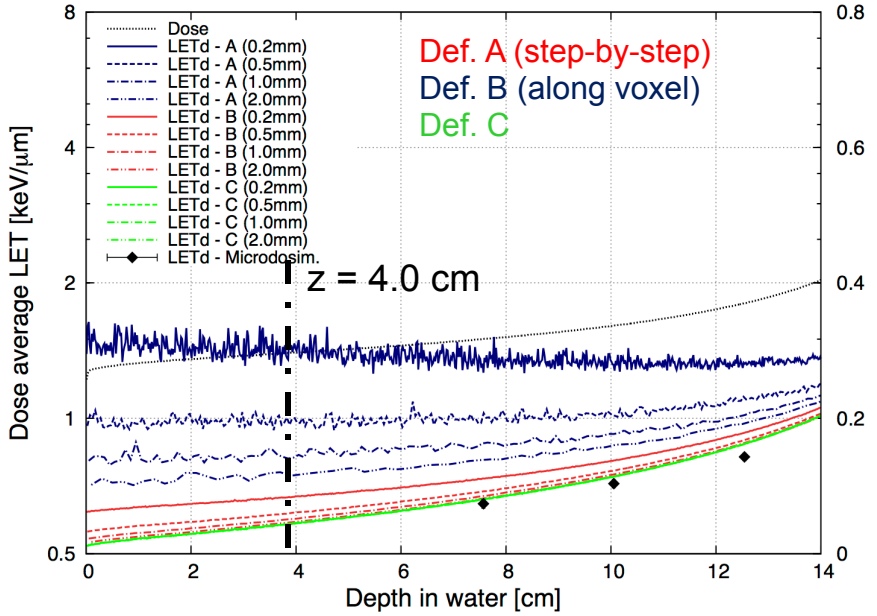

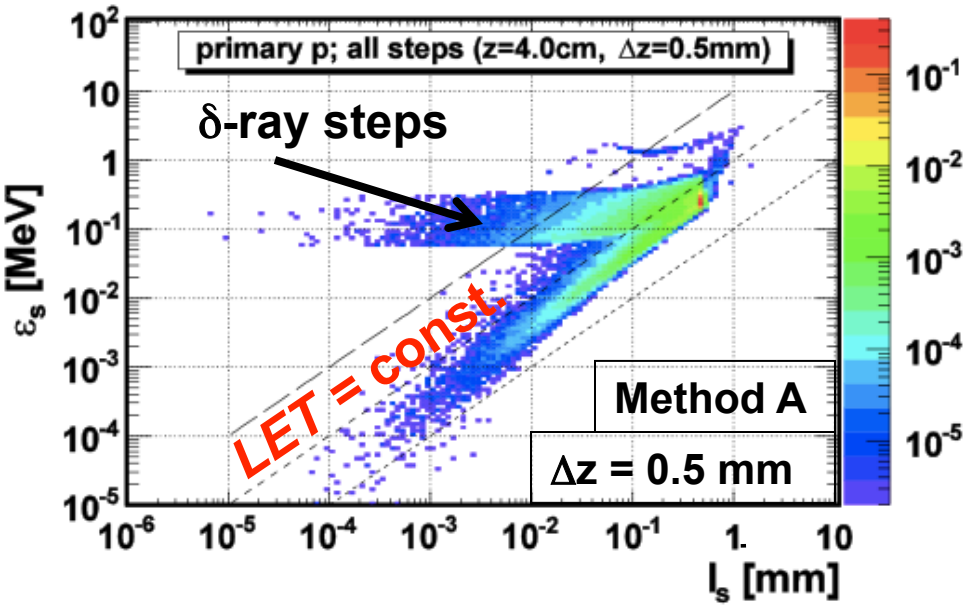

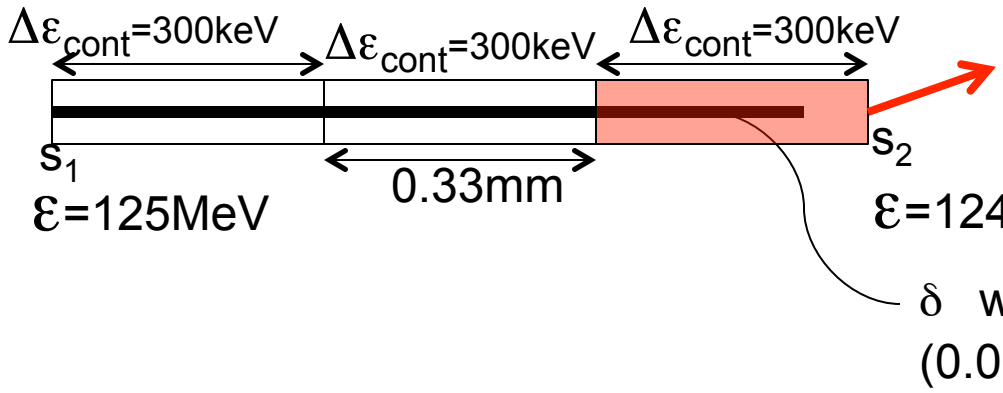

$$L \approx \frac{0.300 + 0.100}{0.33}\frac{MeV}{mm} = 1.21\frac{MeV}{mm}$$

δ with ε=100keV (>0.06MeV)
(0.06MeV = 0.05mm e- range)

Conclusions on LET calculations

- Different monte carlo implementation of LET_d lead to significant deviations in the calculated values, especially at the Bragg Peak region.
- Systematic variations of the calculated LET_d dependant on the voxel size along the beam direction. Its cause is different between entrance and Bragg Peak regions.
- These differences resulted in significant deviations when calculating LET_d distributions for an arbitrary SOBP. (poster)
- Method C recommended for LET_d calculations, as it is independent of voxel size.
- Regardless the method used, calculations need to be contrasted with actual measurements

Microdosimetric Measurements: 3D microdetectors

Work done by: Consuelo Guardiola – University of Pennsylvania & Microelectronic National Center – CSIC (Barcelona)

Soon to be carried out:

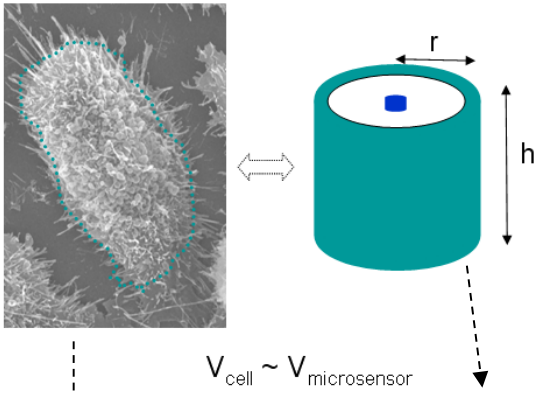

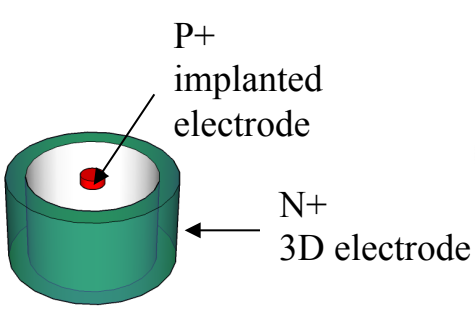

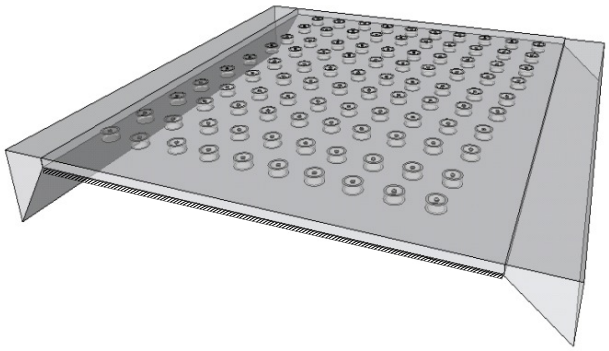

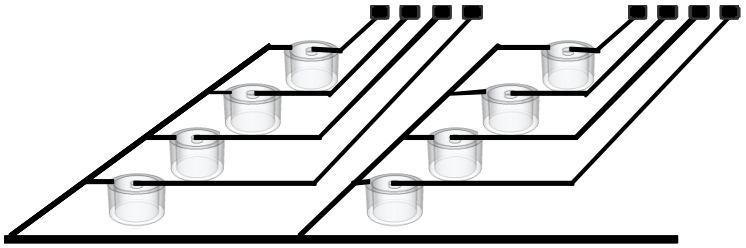

Poster: SU-E-T-380

Microdosimetric Measurements: 3D microdetectors

- **Use IMB-CNM's 3D sensor technology to create cylindrical structures that completely confine the active volume – "cell-like"**
  - P+ implanted electrode surrounded by N+ cylindrical 3D electrode (*trench*)
  - SOI wafer with backside removed to avoid backscattered particles
- Array of independent active volumes with individual (pixel) or serial (strip) readout – spatial resolution
- Patent design approved (2014)
- Fabrication ongoing at IMB-CNM's clean room on 3, 6, 10 and 20 μm SOI wafers.

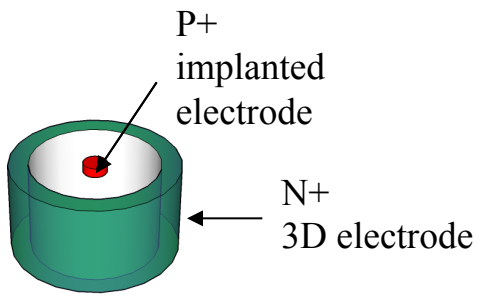

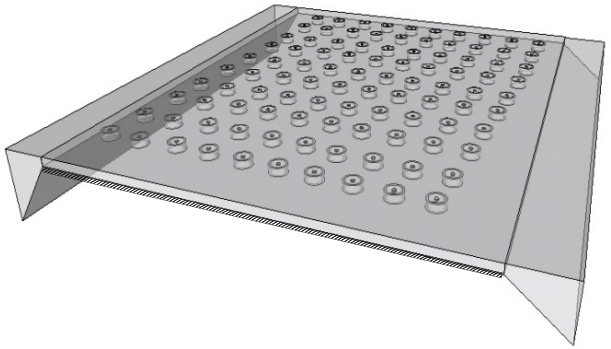

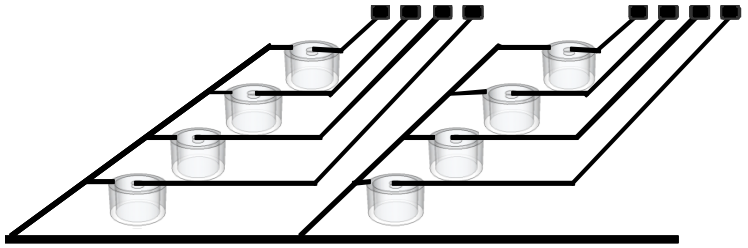

Microdosimetric Measurements: 3D microdetectors

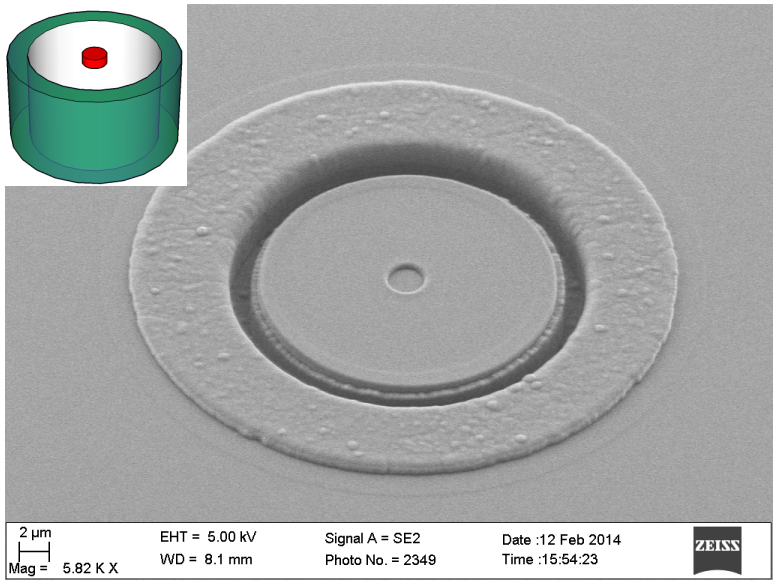

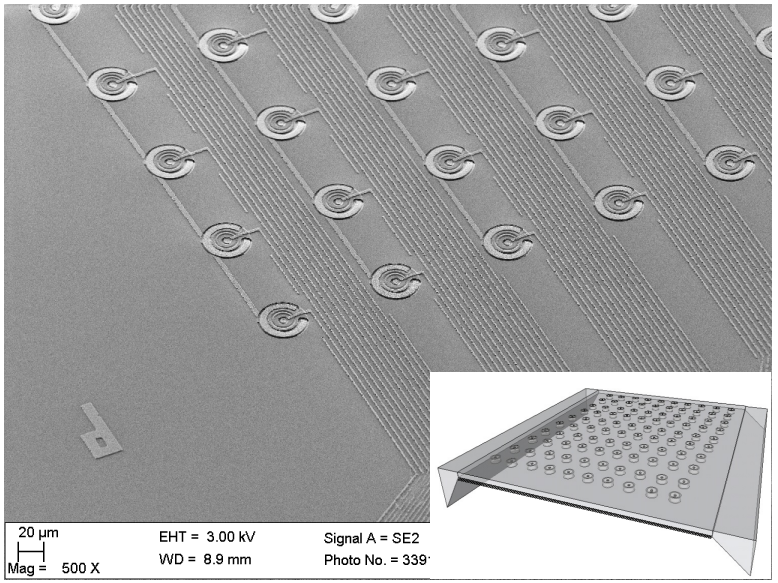

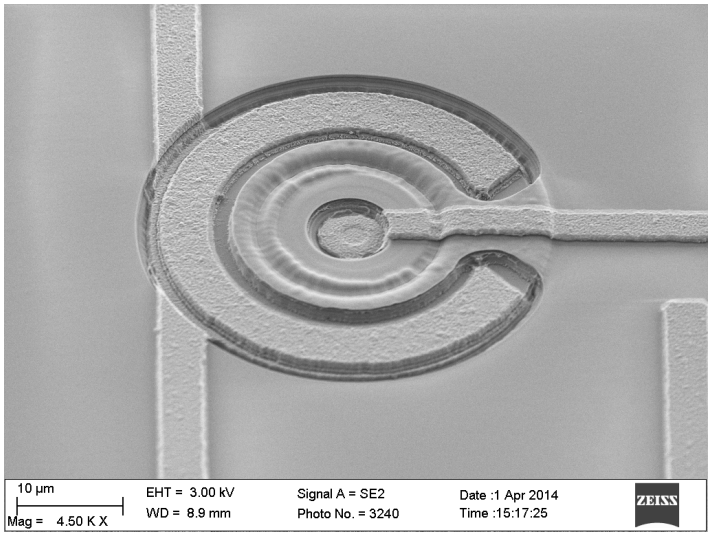

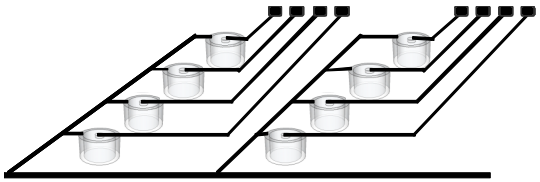

Microdosimetric Measurements: 3D microdetectors

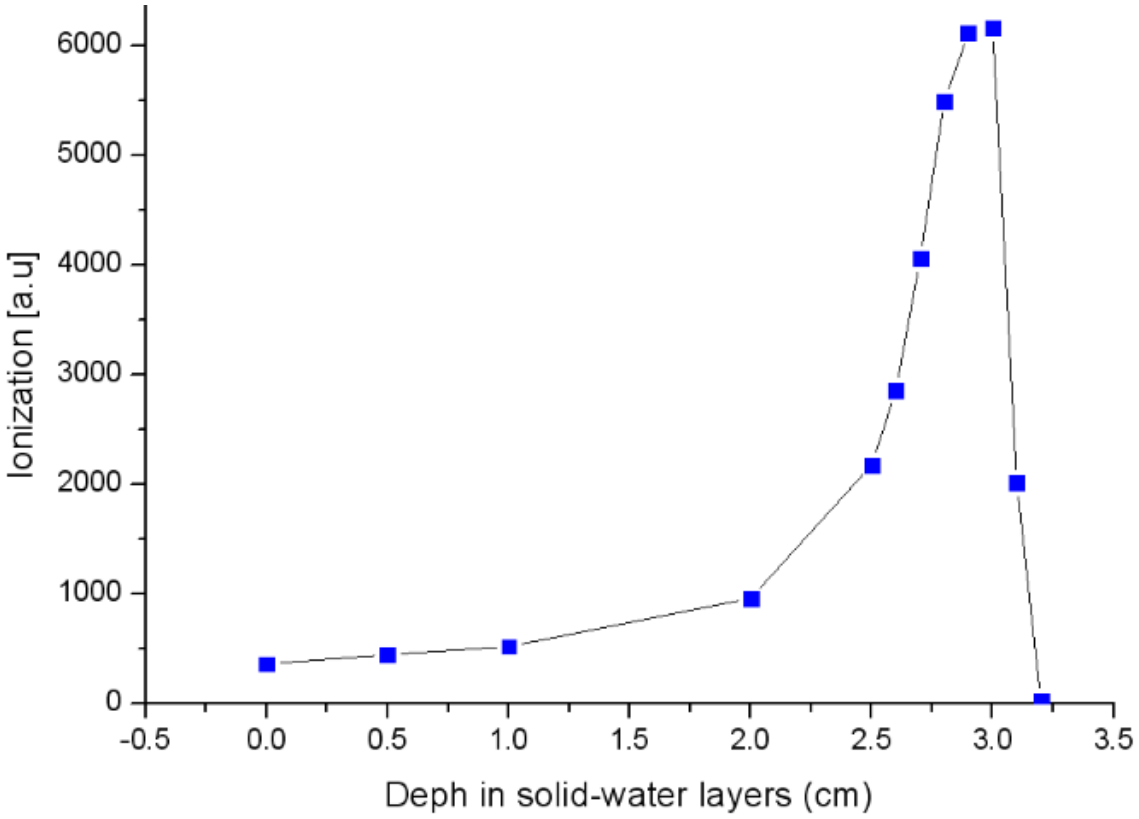

Bragg curve of the 62 MeV proton beam acquired with a solid water phantom with an ultra-thin 3D silicon detector of 10 μm thickness at the Louvain cyclotron

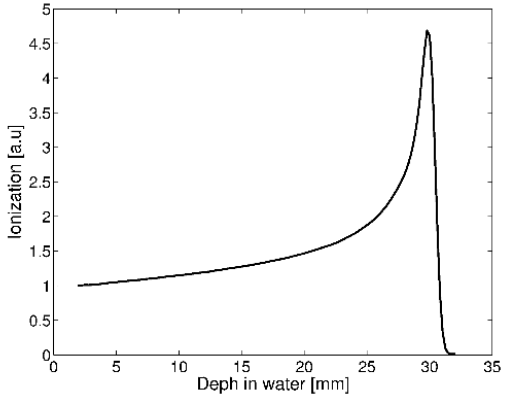

Fig. 5. Bragg peak of 62-MeV proton beam acquired in a water-tank with the Markus ionization chamber at CATANA facility.

*G.A.P. Cirrone et al., IEEE Trans. Nucl. Sci. Vol.51, No.3, 2004

The ultra-thin 3D silicon sensors are reliable for microdosimetry measurements

Microdosimetric Measurements: 3D microdetectors

Pulse height spectra in the water phantom along the Bragg peak

- **10 µm backthinned sensor, 7x7 mm² area**
- **Proton energy 62 MeV, range 32 mm.**
- **Proton flux 10^4 p/cm²s**
- **180 s acquisition**
- **LLD = 90 keV**

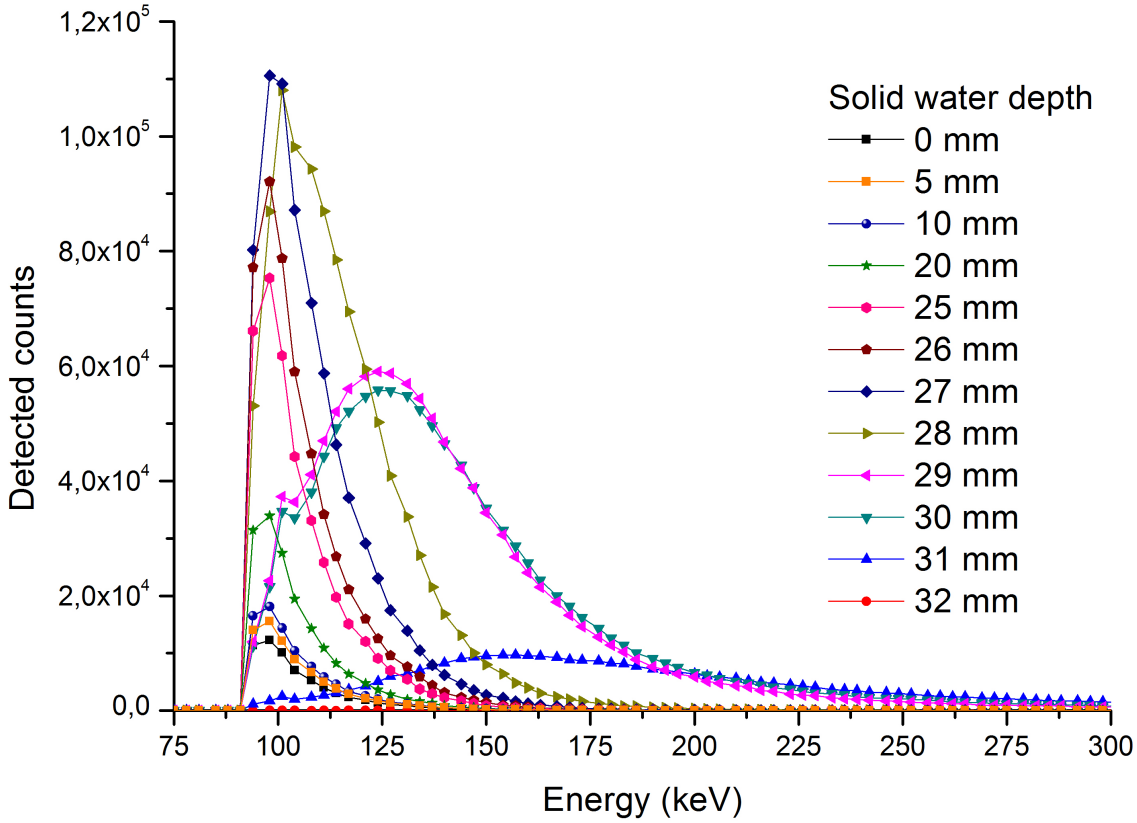

Microdosimetric Measurements: 3D microdetectors

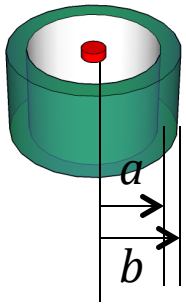

$$l = \frac{2abh}{bh + ab + ah} \Rightarrow \bar{l} = 4\frac{V}{S} \Rightarrow y = \frac{\varepsilon}{\bar{l}} \Rightarrow d(y) = \frac{y\, f(y)}{\overline{y_F}}$$

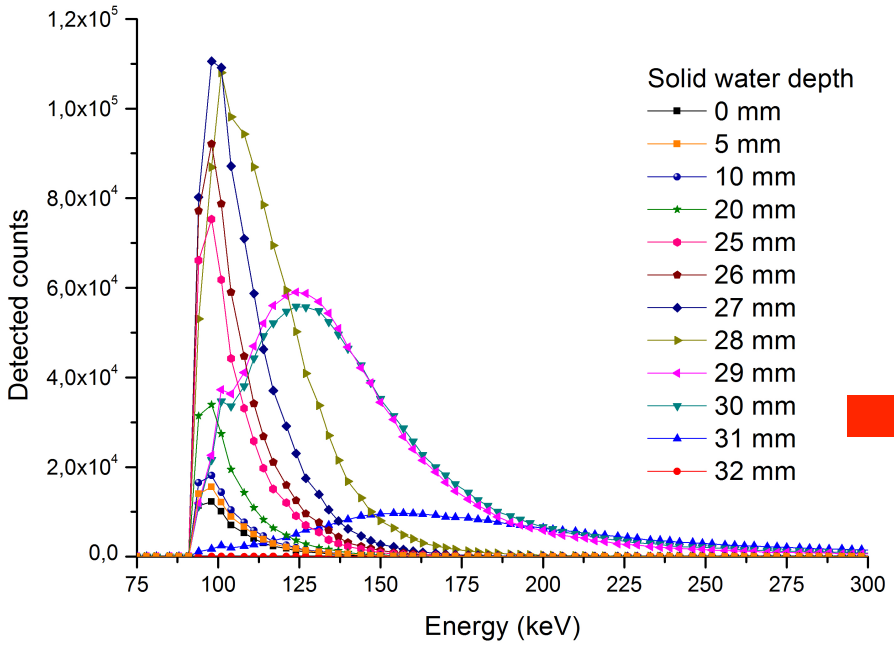

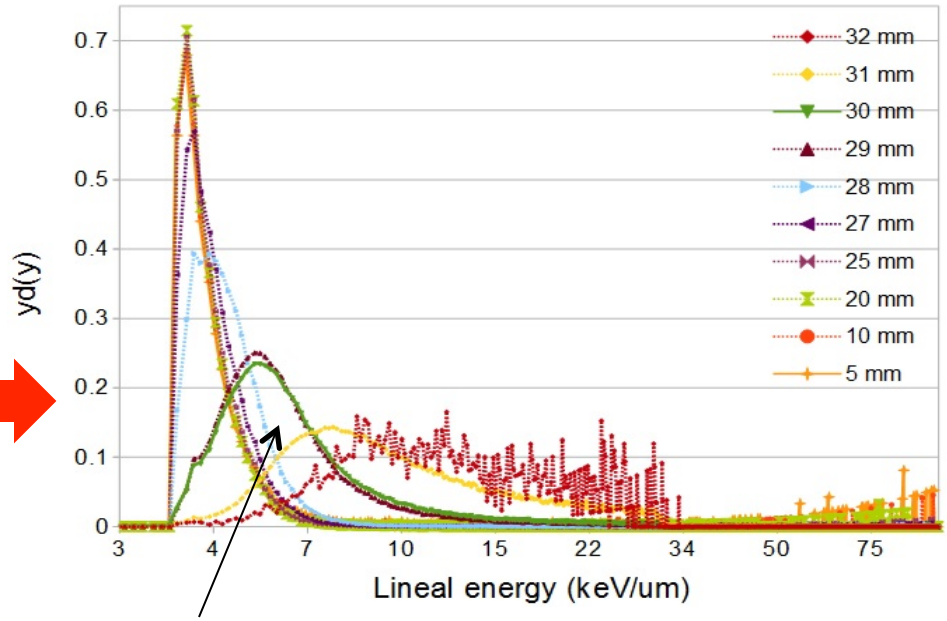

LET ~ average area under the curve

Overall Conclusions

- Radiobiological optimization in particle radiotherapy requires input from many different ‘corners’ to significantly reduce uncertainties
- Full RBE based optimization in proton radiotherapy might still be a premature step, but LET guided treatment planning is doable
- When performing LET based treatment plans, especial considerations must be given to the methodology used to calculate LET
- Calculations of LET must be contrasted with measurements, ie. TPS must be commissioned not only for dose but also for LET. If microdosimetric models are used, TPS cannot rely only on MC calculations but microdosimetric measurements are advisable
- Consideration of LET in proton treatment planning may lead to alternative method of planning still to be fully explored

Overall Conclusions

- **PMAT is an interesting option that might allow simultaneous dose and LET painting of a target while delivering the dose in an efficient manner**

http://youtu.be/L2zdXh3XCdI

Acknowledgements

- Dr Daniel Sanchez-Parcerisa
- Dr Consuelo Guardiola-Salmeron
- Dr Miguel Cortes-Giraldo
- Dr Steve Tuttle
- Mr Marcus Fager
- Mrs Maura Kirk
- Mrs Malorie Stowe
- Mr Brendan Burgdorf
- Mr Mark Kondrla
- Mr Ryan Rue
- Mr Nicole DiGiovanni
- Mr Dan Douglas
- Mrs Alex Shaindlin
- Mrs Oksana Vovchuk
- Prof Tim Solberg
- CNM (Barcelona)